energies

MDPI

Article

Autoregressive Reconstruction of Total Water Storage within GRACE and GRACE Follow-On Gap Period

Artur Lenczuk [1,*], Matthias Weigelt [2], Wieslaw Kosek [3] and Jan Mikocki [1]

[1] Faculty of Civil Engineering and Geodesy, Military University of Technology, 00908 Warsaw, Poland; jan.mikocki@student.wat.edu.pl
[2] Faculty of Civil Engineering and Geodetic Science, Leibniz University Hannover, 30167 Hannover, Germany; weigelt@ife.uni-hannover.de
[3] Department of Geodesy and Spatial Information, Faculty of Production Engineering, University of Life Sciences in Lublin, 20950 Lublin, Poland; wieslaw.kosek@up.lublin.pl
* Correspondence: artur.lenczuk@wat.edu.pl

Abstract: For 15 years, the Gravity Recovery and Climate Experiment (GRACE) mission have monitored total water storage (TWS) changes. The GRACE mission ended in October 2017, and 11 months later, the GRACE Follow-On (GRACE-FO) mission was launched in May 2018. Bridging the gap between both missions is essential to obtain continuous mass changes. To fill the gap, we propose a new approach based on a remove–restore technique combined with an autoregressive (AR) prediction. We first make use of the Global Land Data Assimilation System (GLDAS) hydrological model to remove climatology from GRACE/GRACE-FO data. Since the GLDAS mis-models real TWS changes for many regions around the world, we further use least-squares estimation (LSE) to remove remaining residual trends and annual and semi-annual oscillations. The missing 11 months of TWS values are then predicted forward and backward with an AR model. For the forward approach, we use the GRACE TWS values before the gap; for the backward approach, we use the GRACE-FO TWS values after the gap. The efficiency of forward–backward AR prediction is examined for the artificial gap of 11 months that we create in the GRACE TWS changes for the July 2008 to May 2009 period. We obtain average differences between predicted and observed GRACE values of at maximum 5 cm for 80% of areas, with the extreme values observed for the Amazon, Alaska, and South and Northern Asia. We demonstrate that forward–backward AR prediction is better than the standalone GLDAS hydrological model for more than 75% of continental areas. For the natural gap (July 2017–May 2018), the misclosures in backward–forward prediction estimated between forward- and backward-predicted values are equal to 10 cm. This represents an amount of 10–20% of the total TWS signal for 60% of areas. The regional analysis shows that the presented method is able to capture the occurrence of droughts or floods, but does not reflect their magnitudes. Results indicate that the presented remove–restore technique combined with AR prediction can be utilized to reliably predict TWS changes for regional analysis, but the removed climatology must be properly matched to the selected region.

Keywords: GRACE; TWS; gap; autoregressive method; remove–restore

Citation: Lenczuk, A.; Weigelt, M.; Kosek, W.; Mikocki, J. Autoregressive Reconstruction of Total Water Storage within GRACE and GRACE Follow-On Gap Period. *Energies* **2022**, *15*, 4827. https://doi.org/10.3390/en15134827

Academic Editor: Silvio Simani

Received: 25 May 2022
Accepted: 28 June 2022
Published: 1 July 2022

1. Introduction

For the 2002–2017 period, global monthly changes of terrestrial (or total) water storage (TWS) were provided by the Gravity Recovery and Climate Experiment (GRACE) mission [1]. The GRACE mission yielded new opportunities to analyze the fluctuations in the terrestrial hydrosphere in the form of magnitude of storage and water flow [2]. The GRACE data reflect changes in TWS and changes of the Earth's mantle and lithosphere during earthquakes or Earth's spin axis (GRACE Tellus official website) for nearly two decades. The successor of the GRACE mission, i.e., the GRACE Follow-On (GRACE-FO)

mission, was launched in May 2018 [3], 11 months after the last-available observation was provided by GRACE. Therefore, there exists a gap between these gravity missions which needs to be filled in to obtain global continuous TWS changes.

Aside from the GRACE and GRACE-FO missions, TWS changes can be also observed by other modern satellite missions, such as the Swarm mission [4], data combinations of various missions [5], or observations from a global positioning system (GPS) [6]; all these provide regional or global TWS changes with various spatial and temporal resolutions. Observed changes are frequently compared to hydrological models [7], which provide continuous TWS changes with high spatial resolution—often higher than the nominal resolution of TWS derived from satellite techniques. Current studies prove that hydrological models reliably capture TWS changes [8]. However, due to the mis-modeling of several TWS compartments, hydrological models may sometimes underestimate the magnitude of TWS changes for regions suffering from large surface-water changes or those undergoing an increasing irrigation process [2,9].

Several alternative methods have been proposed to fill the gap between the two GRACE missions. Geodetic observations and geophysical models, such as observations from satellite laser ranging (SLR) [10], the Swarm mission [11], or hydrological models [12] were demonstrated to reasonably reconstruct 11 missing months of TWS changes; they all provide physical information about TWS changes. In contrast, mathematical and statistical approaches, although containing no physical information, were also proven to reasonably fill the GRACE and GRACE-FO gaps [13]. To include physical information into TWS reconstruction, mathematical algorithms were either modified with meteorological parameters [14,15] or trained with SLR data [16], with only GRACE data [17], with GRACE and Swarm data [18], or with a combination of satellite data with meteorological/hydrological parameters [19,20], and were demonstrated to correlate well with GRACE [21,22]. The main advantage of mathematical approaches is that they are able to predict climate signals such as droughts [23] or floods [24] to reconstruct signals of the El Niño oscillation [22] or human-induced TWS changes [25] at any spatial resolution. However, observations also have their constraints (limited spatial or temporal resolution) by which they are unable to correctly reflect the aforementioned changes in water storage. For example, using solely data provided by the GRACE mission, we are unable to make a reliable assessment of monthly TWS changes for areas smaller than 150,000 km^2. However, using mathematical methods or meteorological parameters, it is possible to obtain higher spatial [26] and temporal resolutions [27] for GRACE data. At present, no recommendation has yet been specified regarding whether physical or mathematical approaches should be used to fill the GRACE gap. Hence, the estimation of TWS changes for the missing 11 months is still an open question for scientists.

Many mathematical methods have been already presented to predict global TWS changes. Simple linear regression can be used alone, or can be supported by seasonal signals to reasonably capture TWS changes observed by GRACE. Both regression methods are applicable to individual TWS time series and ignore spatial dependencies between TWS changes. To overcome this issue, more comprehensive mathematical algorithms, such as multichannel singular spectrum analysis (MSSA), were proposed [28]. To fill the gap between the GRACE and GRACE-FO missions, autoregressive (AR) models were also applied and demonstrated to predict future TWS changes better than a simple linear regression model [29]. Moreover, GRACE-derived TWS values correlate better with AR-predicted values than with hydrological models for a river basin scale [22]. In addition, AR prediction performs better than the multiple linear regression models for dry and intensively irrigated regions [29]. For example, the future long-term groundwater changes in the Colorado river basin can be effectively predicted by AR-like models [13], which is a huge advantage over hydrological models, whose long-term trends are always underestimated.

The observation gap between the GRACE and GRACE-FO missions considerably impede the complete analysis and full exploitation of the data. Despite previous tests to solve the gap-filling problem, a recommended approach is still lacking. Here, we

present a new way to reconstruct the TWS changes for 11 months and, bridging the gap between the GRACE and GRACE-FO missions, to reconstruct data from both missions, based on an AR model. Since AR prediction requires that time series be stationary, we remove climatology from the GRACE and GRACE-FO data using a hydrological model. We then apply a simple least-squares estimation (LSE) to remove remaining deterministic signals. A two-step approach is necessary because of not including geophysical effects in the LSE (use of hydrological model) and the underestimation of GRACE-observed climatology by hydrological models (especially trends; use of LSE). Residuals are then subjected to the AR prediction process. Unlike the previous estimates, our AR prediction process of TWS residuals is performed for the GRACE and GRACE-FO data. The GRACE data are used to predict TWS residuals forward, while the GRACE-FO data are used for the first time to perform backward prediction. This is possible since no intermission bias exists between both missions [3]. Both estimates meet right in the middle of a gap period and the magnitudes of misclosures are estimated. Then, to obtain continuous TWS series of residuals, the magnitudes of misclosures are divided into equal halves and dispersed for forward- and backward-predicted values. Since LSE and hydrology signals can be added back to finally estimate the predicted GRACE and GRACE-FO TWS changes, our approach is named the remove–restore technique. Our results showed that the proposed remove–restore technique provides new opportunities to fill in GRACE observations and allows assessing the complete analysis of water storage, including land hydrology, from GRACE satellites. We notice that the proposed method helps to overcome some problems and limitations (especially for other satellite geodetic techniques) while bridging the GRACE/-FO gap, e.g., (1) the size of regions (spatial or temporal resolution, i.e., Swarm [10] or combined HLSST data [30], or (2) the underestimation of real changes' magnitude for approaches based on hydrological models [12]. For example, compared to other reconstruction approaches, we overcome the temporal limitations of the study presented by [17] (data available through December 2016) or availability and resolution data provided by [22] (data for 26 river basins through December 2018). Moreover, we would like to propose that our method can be used to fill in other kinds of data gaps, not only for GRACE-type data.

The paper presents the dataset and methodology in Sections 2 and 3, respectively. Results are presented and discussed in Section 4. Section 5 summarizes the main findings.

2. Datasets

2.1. GRACE and GRACE Follow-On Data

We use TWS changes provided in a form of Release-06 (RL06) mascon solution by the Center for Space Research (CSR) in Austin, USA [31], which are recommended by GRACE Tellus official website. We employ 196 months of TWS changes observed by the GRACE (163 months) and GRACE-FO (33 months) missions, for the period of April 2002–April 2021, summing into 19 years of data with an 11-month gap between the two missions in the period between July 2017 and May 2018. (Both the GRACE and GRACE-FO missions are abbreviated further with GRACE/-FO.) TWS changes within mascons are modeled using the global distribution of mass concentration blocks in a finite time interval in a relation to the mean gravity field. In comparison to traditional spherical harmonic functions, mascons are based on more rigorous empirical methods [31], which are used to remove north–south stripes and reduce leakage effects between land and ocean grids [31]. Consequently, mascons contain higher variance of signals than spherical harmonic solutions for corresponding degrees and orders [32]. Mascons are defined within the range of 89.875° N/S for latitude and within the range of 0.125° to 359.875° E for longitude. We average the TWS values, provided originally in a 0.25° × 0.25° grid, to a 1° × 1° grid, which is argued as the native resolution of CSR RL06 mason solution (CSR official website).

2.2. GLDAS Hydrological Model

We use the Global Land Data Assimilation (GLDAS) hydrological model [33], being one of the land surface models (LSMs). GLDAS is constructed on the basis of a new generation of high-resolution ground-based and space observation systems at a higher temporal and spatial resolutions. GLDAS provides hydrological data using four different LSMs, which mainly differ in the technical parameters of the delivered products, e.g., the depth of soil moisture layers. From the variety of GLDAS models, the Noah version is characterized by the highest consistency with GRACE data [28]. We, therefore, use monthly TWS changes from the Noah GLDAS 2.1 [34] hydrological model, which are available from January 1979 until present on a $1^\circ \times 1^\circ$ grid. We employ 19 years' (229 months') worth of GLDAS TWS changes, for the period of April 2002 to April 2021, to be consistent with the GRACE/-FO runtime. We also use observations within the GRACE/-FO gap. The utilized GLDAS TWS grid constitutes the sum of canopy, snow water storage, and soil moisture components. The GLDAS model does not contain the ice and glacier components, so the Greenland and Antarctica regions are excluded from our analysis.

2.3. WGHM Hydrological Model

We used the WaterGAP Global Hydrological Model (WGHM) [35], being one of the global hydrological and water resource models (GHWRMs). The WGHM focuses on freshwater flow and water content changes for five different factors that cause uncertainties, i.e., climate modeling, land cover, model structure, human water use, and data calibration, against water exchange in rivers. WGHM also contains information about anthropogenic impacts to water storage, i.e., irrigation, animal breeding, household water usage (households and small businesses), industry, and power plant layers, from five different global models, which are defined as the WGHM TWS grid. The TWS is the sum of canopy, snow water storage, soil moisture, groundwater, and surface water components. We use an updated WaterGAP 2.2d version based on the climate dataset defined in the Global Soil Wetness Project (GSWP3) and generated using the WATCH Forcing Data (WFD) methodology, applied to surface meteorological variables from the ERA5 reanalysis (WFDE5, personal contact). Data are available from January 1901 until December 2019 on a $0.5^\circ \times 0.5^\circ$ grid. We used 213 months' worth of TWS changes, from April 2002.

2.4. Swarm Data

The alternative gravity field variations to the GRACE/-FO mission are provided by the ESA's Earth's Magnetic Field and Environment Explorer (Swarm) mission [36], which was launched in November 2013; we employ 89 months' worth of observations for the period of December 2013–April 2021, generated by the Combination Service of Time-variable Gravity Fields (COST-G) [7]. The Swarm observations are provided in the form of spherical harmonics, and Swarm TWS changes are estimated similar to GRACE/-FO spherical harmonic data [37]. Swarm data are available at the International Center for Global Earth Models (ICGEM) official website to a degree and order of spherical harmonics up to 40. However, due to excessive noise in the higher-harmonics one, we truncated them and used only harmonics for a degree and order up to 12 (which corresponds to a spatial resolution of 3000–4000 km). Moreover, to be consistent with the GRACE data, the same background models for the Swarm processing were defined.

3. Methodology

Previous works using an AR process to fill the gap between the GRACE/-FO missions were directly based on forecasting the total signal, i.e., total TWS changes [22,29], or a singular TWS component such as groundwater [13]. Since seasonal signals dominate other contributors in TWS changes for many regions [38], the predicted values were dominated by annual and semi-annual changes. Therefore, sub-seasonal and inter-annual changes were hardly noticeable (i.e., [11]). We propose a novel AR prediction grounded on residuals,

which enables the evaluation of long-term inter-annual and sub-seasonal signals occurring in the TWS time series.

Our method is based on the remove–restore technique and consists of several steps (Figure 1). First, we use the GLDAS hydrological model to remove climatology from the GRACE/-FO TWS changes. In this way, we obtain TWS differences, from which remaining deterministic signals are removed based on an LSE algorithm. The proposed approach, where climatology is removed in two steps (hydrological model and LSE), allows us to (1) include geophysical effects, which LSE does not capture (climatology from a hydrological model is used), and (2) remove trends and seasonality, which are underestimated by models (climatology from the LSE method is used). Then, TWS residuals are subjected to the AR prediction process. Full residuals with no gaps inside are named predicted TWS residuals. To these residuals, deterministic signals and GLDAS TWS changes can be added back, to finally end up with predicted GRACE/-FO TWS changes. Details of the individual algorithms are provided below.

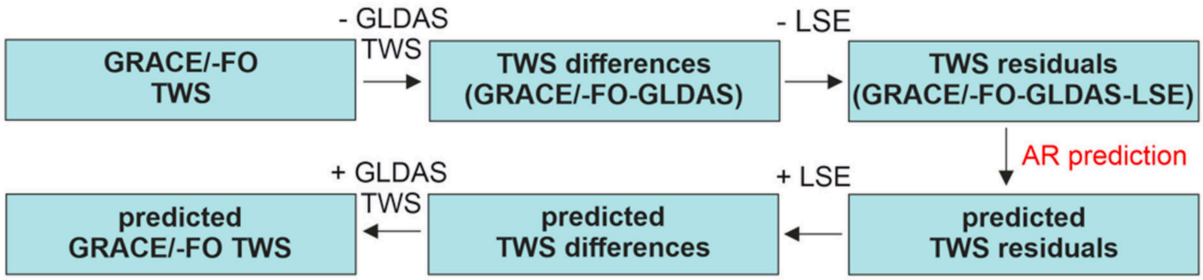

Figure 1. Flowchart of the methodology. We use the remove–restore technique. GRACE/-FO means GRACE and GRACE Follow-On datasets, LSE stands for the least-squares estimation, AR for the autoregressive process, and TWS for total water storage. We remove climatology from the GRACE data by using the GLDAS TWS changes, and obtain the TWS differences. Then, we apply LSE to remove all remaining deterministic signals mis-modeled in the GLDAS, obtaining the TWS residuals. These are then subjected to AR prediction and called predicted TWS residuals. Once the prediction is performed, the LSE deterministic model could be added back (predicted TWS differences) along with the GLDAS TWS changes. In this way, we obtain predicted GRACE/-FO TWS changes.

LSE is used to provide the estimates of trends and annual and semi-annual signals within each grid node. For this purpose, we employ the following time series model of TWS changes:

$$TWS(t) = TWS_0 + b \cdot t + \sum_{i=1}^{2} [S_i \cdot \sin(\omega_i t) + C_i \cdot \cos(\omega_i t)] + res \quad (1)$$

where $TWS(t)$ is a modeled TWS time series for t, TWS_0 is the TWS value for t_0, b means trend, S_i and C_i are the sine and co-sine amplitudes of the annual and semi-annual components, and res represents the TWS residuals. After removing the deterministic components using the LSE method, the time series of the obtained TWS residuals are subjected to the AR prediction process.

An autoregressive AR(M) model of zero-mean stationary stochastic process x_t is expressed as:

$$x_t = a_1 x_{t-1} + a_2 x_{t-2} + \ldots + a_M x_{t-M} + n_t \quad (2)$$

where M is the autoregressive order, n_t is a white noise process with a variance σ_n^2, and $a_1, a_2, a_3, \ldots, a_M$ are the autoregressive coefficients. A forecast based on the autoregressive model uses a linear combination of past values of the variable and their forecasts [39]:

$$\begin{array}{c} \hat{x}_{N+1} = \hat{a}_1 x_N + \hat{a}_2 x_{N-1} + \ldots + \hat{a}_M x_{N-M-1} \\ \hat{x}_{N+2} = \hat{a}_1 \hat{x}_{N+1} + \hat{a}_2 x_N + \ldots + \hat{a}_M x_{N-M-2} \\ \ldots \\ \hat{x}_{N+L} = \hat{a}_1 \hat{x}_{N+L-1} + \hat{a}_2 \hat{x}_{N+L-2} + \ldots + \hat{a}_M x_{N-M-L} \end{array} \quad (3)$$

where N is the total number of data used to estimate the autoregressive coefficients, L is the maximum prediction length, $\hat{a}_1, \hat{a}_2, \ldots, \hat{a}_M$ are the estimations of the autoregressive coefficients, and $\hat{x}_k : k = N+1, \ldots, N+L$ are prediction estimates.

Assuming that the TWS residuals are stationary, the main problem with the use of the autoregressive model is to determine the autoregressive order M. Too-low autoregressive orders are not able to reliably model long-term changes, while too-high autoregressive orders may result in additional correlations in the high-frequency band of a stochastic process. To estimate an optimum order, we use Akaike's information criterion [40], namely:

$$AIC(M) = \ln \hat{\sigma}_n^2(M) + \frac{2M}{N} = \min \quad (4)$$

where $\hat{\sigma}_n^2(M) = \hat{c}_0 - \hat{a}_1 \hat{c}_1 - \hat{a}_2 \hat{c}_2 - \ldots - \hat{a}_M \hat{c}_M$ is the estimation of the noise variance based on the M parameter model. Autoregressive coefficients are estimated using LSE as follows:

$$\begin{pmatrix} \hat{a}_1 \\ \hat{a}_2 \\ . \\ \hat{a}_M \end{pmatrix} = \begin{pmatrix} \hat{c}_0 & \hat{c}_1 & . & \hat{c}_{M-1} \\ \hat{c}_1 & \hat{c}_0 & . & \hat{c}_{M-2} \\ . & . & . & . \\ \hat{c}_{M-1} & \hat{c}_{M-2} & . & \hat{c}_0 \end{pmatrix}^{-1} \begin{pmatrix} \hat{c}_1 \\ \hat{c}_2 \\ . \\ \hat{c}_M \end{pmatrix} \quad (5)$$

where $\hat{c}_k = \frac{1}{N} \sum_{t=1}^{N-k} x_t x_{t+k}$ is the biased autocovariance estimate.

The process of forecasting 11 months of missing TWS changes is based on backward and forward predictions. Forward AR prediction is performed based on the TWS residuals before the gap (GRACE data; the forward approach). Backward AR prediction is based on the TWS residuals after the gap (GRACE-FO data; the backward approach). Our prediction of 11 months' worth of missing TWS residuals needs to be tied to real TWS residuals. Therefore, we remove the last observations from GRACE (June 2017) and the first observations from GRACE-FO (May 2018) and start the prediction from the previous value, i.e., from May 2017 in the forward approach and from May 2018 in the backward approach. By doing so, we eliminate the possible shift of the predicted TWS residuals.

To use the autoregressive method for the TWS residuals' prediction process, the time series have autocorrelations themselves. Thus, to check the correlation between individual values of TWS residuals series, we employ the autocovariance function of TWS residuals computed separately for GRACE and GRACE-FO data for all continental grid nodes (Figure 2). The values presented in Figure 2 show that the GRACE and GRACE-FO TWS residuals are correlated and are mainly characterized by seasonality of approximately one year.

The autocovariance function is also used to estimate the optimal length of the time series (a number of months) for constructing the AR model. We find that the autocovariance function comes close to neglectable values for a time lag of 24 months. Therefore, we assume the number of 24 months as the optimum data length to determine the AR model. Adopting the same length of time series to define the AR models for both the GRACE and GRACE-FO data enables us to obtain similar accuracy between the forward and backward forecasts. We also test the impact of adopting a longer time series to construct the AR model. We adopt the number of 33 months (the length of GRACE-FO data) and find that the predicted values

degrade by 10–15% when longer time windows are utilized. Figure 2 presents the values of the autocovariance function for the GRACE (Figure 2a) and GRACE-FO (Figure 2b) time series with a length equal to 33 months (the number of used monthly observations from the GRACE-FO mission). The plots for both missions are similar. It can be seen that, mainly, both autocovariance series decrease with time in the beginning. We notice that, for both missions, the autocovariance values converge to zero near the 24-months point. However, after a time of 10 months, the autocovariance slightly increases, to 0.4×10^6 mm and 0.2×10^6 mm for GRACE and GRACE-FO, respectively. The maximum values are obtained at 1 month in both cases. The minimum values are near -0.4×10^6 mm, in a range between 5–10 months and 10–20 months for the GRACE and GRACE-FO series, respectively. A comparison of these two missions reveals that GRACE-FO data exhibits smaller autocovariances in general.

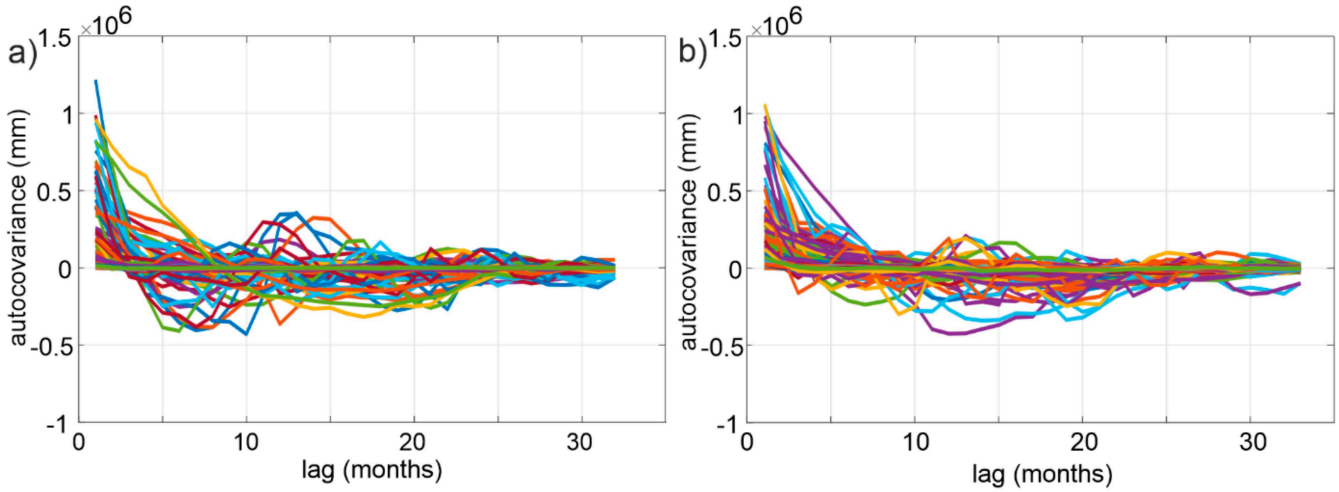

Figure 2. Autocovariance of TWS residuals estimated for 33 months for the (**a**) GRACE and (**b**) GRACE-FO missions.

In the case of the forward- and backward-predicted time series, there may be a situation where the time series do not merge. We describe this as a misclosure and estimate for the mid-gap period. To receive continuous time series of TWS changes, we artificially make these two ends meet. To do this, we scatter half of the misclosures for both forward- and backward-predicted time series. The misclosures were added to each month gap proportional to the number of months calculated from the last month of GRACE (forward approach) or the first month of GRACE-FO (backward approach) to the mid-gap month. This means that half of the misclosures is divided by the number of months it will be added to. For instance, if a misclosure is equal to 10 cm, we divide it into halves, i.e., 5 cm. Then, that 5 cm half is divided by the number of months for which the prediction is estimated, counting from the mid-gap month, i.e., 5 cm/1, is added to the mid-gap month, 5 cm/2 is added to the previous month, etc.

In the following study, to assess the quality of the presented prediction methods, we determine a few statistical measures. Firstly, to assess the ability of the adopted climatology to predict the GRACE/-FO TWS changes, we estimated the Nash–Sutcliff efficiency (NSE) [41] coefficient by using:

$$\mathrm{NSE} = 1 - \left[\frac{\sum_{i=1}^{n} (\mathrm{GRACE/-FO\ TWS}_i - \mathrm{model\ TWS}_i)^2}{\sum_{i=1}^{n} \left(\mathrm{GRACE/-FO\ TWS}_i - \overline{\mathrm{GRACE/-FO\ TWS}} \right)^2} \right] \quad (6)$$

where n is the number of observations and is equal to 196 months of GRACE/-FO data, and model TWS_i means TWS changes provided by the GLDAS or WGHM hydrological

model. Secondly, to assess the quality of the reconstructed signals, we estimate the latitude-weighted mean absolute error (MAE, Equation (7)) and the latitude-weighted root-mean-squared error (RMSE, Equation (8)) as follows [28]:

$$\mathrm{MAE}(\Omega) = \sqrt{\frac{\sum\limits_{\forall i \in \Omega} \left(\left| \text{GRACE TWS}_i - \text{predicted GRACE TWS}_i \right| \cdot \cos \varphi_i \right)}{\sum\limits_{\forall i \in \Omega} \cos \varphi_i}} \tag{7}$$

$$\mathrm{RMSE}(\Omega) = \sqrt{\frac{\sum\limits_{\forall i \in \Omega} \left(\left(\text{GRACE TWS}_i - \text{predicted GRACE TWS}_i \right)^2 \cdot \cos \varphi_i \right)}{\sum\limits_{\forall i \in \Omega} \cos \varphi_i}} \tag{8}$$

where φ_i is the latitude and Ω represents a specific range of selected regions, e.g., Amazon, Northern Territory of Australia, or Central Europe. All i nodes within Ω are summed based on their area weighted by latitudes.

4. Results and Discussion

4.1. Selection of the Optimal Order of the Autoregressive Model

Firstly, we focus on determining the optimal order for the autoregressive model. The autoregressive order M was estimated from the TWS residual time series. In Figure 3, we show the global autoregressive order values for the TWS residuals obtained after reducing the GRACE/-FO TWS by the GLDAS TWS. We note that order M is a range between four and six for the forward (Figure 3a) and backward (Figure 3b) approach. We show that for nearly 40% of continental grid nodes, an autoregressive order M equal to five is preferred for the TWS residuals. Therefore, we employ an order equal to five and assume that it is optimal for all TWS residuals. To assess the reliability of our results estimated based on the GLDAS as climatology, we used also the WGHM. For the WGHM model, we obtained an autoregressive order M equal to five for a similar number of stations (Table 1).

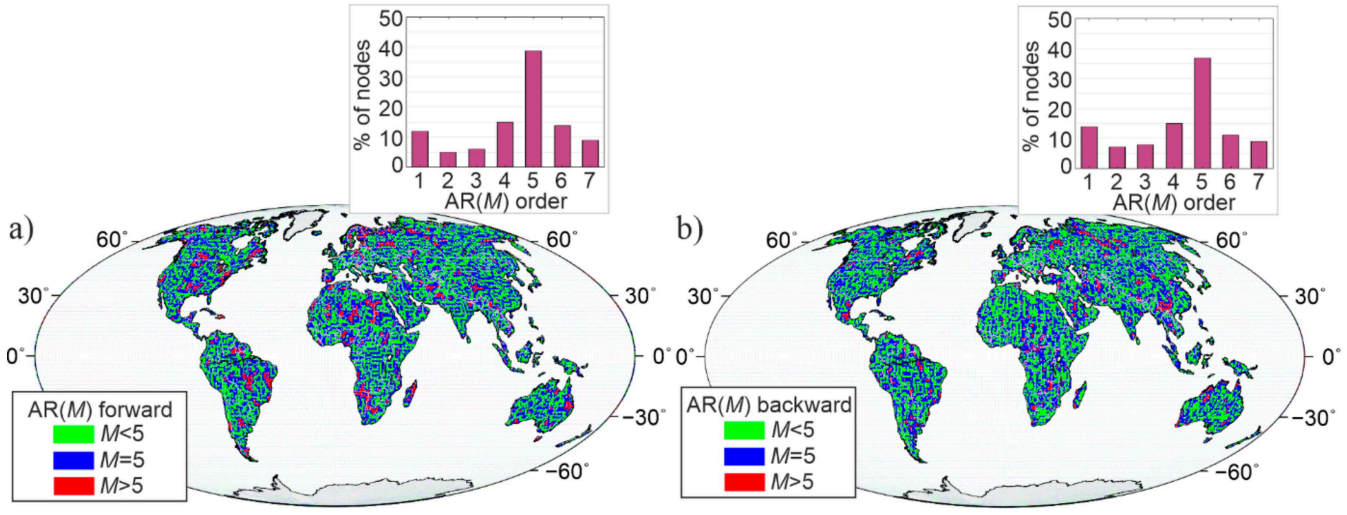

Figure 3. Maps present autoregressive order M estimated for TWS residuals for the (**a**) forward and (**b**) backward approach, where green, blue, and red reflect regions characterized with order M smaller, equal to and greater than 5, respectively. Bar graphs present the percentage of all $1^\circ \times 1^\circ$ continental grid nodes for each autoregressive order M.

Table 1. Autoregressive order for TWS residuals estimated for the GRACE/-FO and GLDAS/WGHM hydrological models with percentage of continental grid nodes.

Autoregressive Order	% of Continental Nodes			
	GLDAS		WGHM	
	Forward	Backward	Forward	Backward
$M < 5$	38	44	45	43
$M = 5$	39	36	38	36
$M > 5$	23	20	17	21

We obtained a similar number of nodes for order $M < 5$ for the GLDAS and WGHM models. We received 38%, 44% nodes for the forward and 45%, 43% nodes for the backward approaches for GLDAS and WGHM, respectively. We show the spatial divergence of the M values in Figure 3 for the GLDAS model, along with graphs representing the percentages of nodes for each M from 1 to 7 for the forward (a) and backward (b) approaches. It shows that the spatial distributions of the autoregressive order M are similar for both approaches. The $M < 5$ (green regions) and $M = 5$ (blue regions) estimated for the gridded nodes are dominant in each continent for both prediction approaches (Figure 3). The $M > 5$ (red regions) are found mainly in the central parts of Africa, Asia, and South America for both prediction approaches, and in Northern Europe and the central part of North America for only the forward approach. Analyzing the M values (graphs in Figure 3) estimated for each node, M values equal to 1, 4, and 6 also dominate, and the graphs have a similar shape (Figure 3) for both approaches. For the WGHM model, the spatial distribution and the number of nodes for each M are almost identical (the maximum differences equal to $\pm 4\%$). Therefore, the results estimated for the WGHM model are not presented.

4.2. Comparison of TWS Changes between GRACE/-FO and Hydrological Models

To select the optimal hydrological model to remove climatology from GRACE/-FO, we compare the TWS of GRACE/-FO with the TWS defined in the GLDAS and WGHM models. Firstly, to assess their effectiveness with respect to GRACE/-FO, we estimate the Pearson correlation coefficient between the TWS changes estimated from the GRACE/-FO and GLDAS hydrological model (Figure 4a) with a 95% confidence level (Figure 4b). We note the positive correlation coefficients for 85% of areas and the correlation coefficients greater than 0.5 for 65% of regions. We also note regions, such as North Africa, Central Asia, or the Arabian Peninsula, for which the TWS changes from the GRACE and GLDAS are uncorrelated with each other. For these regions, a poor correlation between the TWS changes from GLDAS and GRACE/-FO may be explained by a lack of availability of observations employed for the generation of the GLDAS model. Therefore, some TWS changes, observed by GRACE-FO, may be mis-modeled within the GLDAS model. Areas of poor correlation are mostly characterized by insignificant correlation coefficients (Figure 4b). In the case of WGHM, the spatial distribution of correlation coefficients (Figure 4d) is similar to GLDAS (Figure 4a), but we obtained lower correlations mainly in the central and southern part of Africa, the central part of North America, in South Asian regions, and in Australia. This confirms the waning contribution of surface water to the total TWS signal (GLDAS does not contain a surface water component); this has been shown already by [42]. We received a positive correlation for 77% of grid nodes for WGHM and correlation greater than 0.5 for 4% of nodes, less than for GLDAS. The calculated coefficients are insignificant for twice as many nodes compared to GLDAS (Figure 4b,e), particularly in central North America, western South America, South Africa, central Asia, and Australia (Figure 4e). To further examine the consistency between GRACE/-FO and the hydrological models, we estimate the NSE coefficient (Figure 4c,f) by using Equation (6). NSE can range between $-\infty$ and one. Values equal to one stand for a perfect fit between TWS changes from hydrological models and GRACE/-FO, while coefficients lower than zero indicate that the mean value of TWS changes derived from GRACE/-FO is a better predictor of

TWS changes than hydrological models. Values of NSE coefficient larger than 0.7 can be interpreted as a very good fit between GRACE/-FO and models [43]. In other words, the NSE efficiency coefficients indicate how well the observed and modeled TWS changes fit the 1:1 line. For most inland areas, the spatial distribution of NSE coefficients is similar to the spatial distribution of correlation coefficients (compare Figure 4a,c). We note that most regions are characterized by a very good fit of the GLDAS hydrological model to GRACE/-FO (NSE coefficients larger than 0.7). At the same time, there are areas, for which NSE coefficients are negative, such as central parts of Australia and Asia, and Africa, for which the GLDAS hydrological model has no predictive skills of the GRACE/-FO TWS changes. For the WGHM model (Figure 4f), we obtained larger divergences for the NSE coefficients parameter than for GLDAS (Figure 4c), especially for regions located in North America, the north part of Africa, and Asia that are characterized by a negative NSE. We obtained, for 5% of nodes, more NSE values less than −1 for WGHM than for GLDAS. The statistical measures for GRACE/-FO and both hydrological models are presented in Table 2.

Now, we use the TWS differences, i.e., the differences between the GRACE/-FO TWS changes and the TWS changes from the GLDAS and WGHM hydrological models. Since we know that hydrological models are not efficient to reflect the TWS changes from GRACE/-FO all over the world, we assume that TWS differences may still contain deterministic signals which may hamper the AR prediction process. Therefore, we estimate the remaining deterministic parameters mis-modeled within the GLDAS and WGHM hydrological models by using a simple LSE method, i.e., Equation (1). We assume trend, annual, and semi-annual components. This procedure is aimed at the further widening of TWS differences.

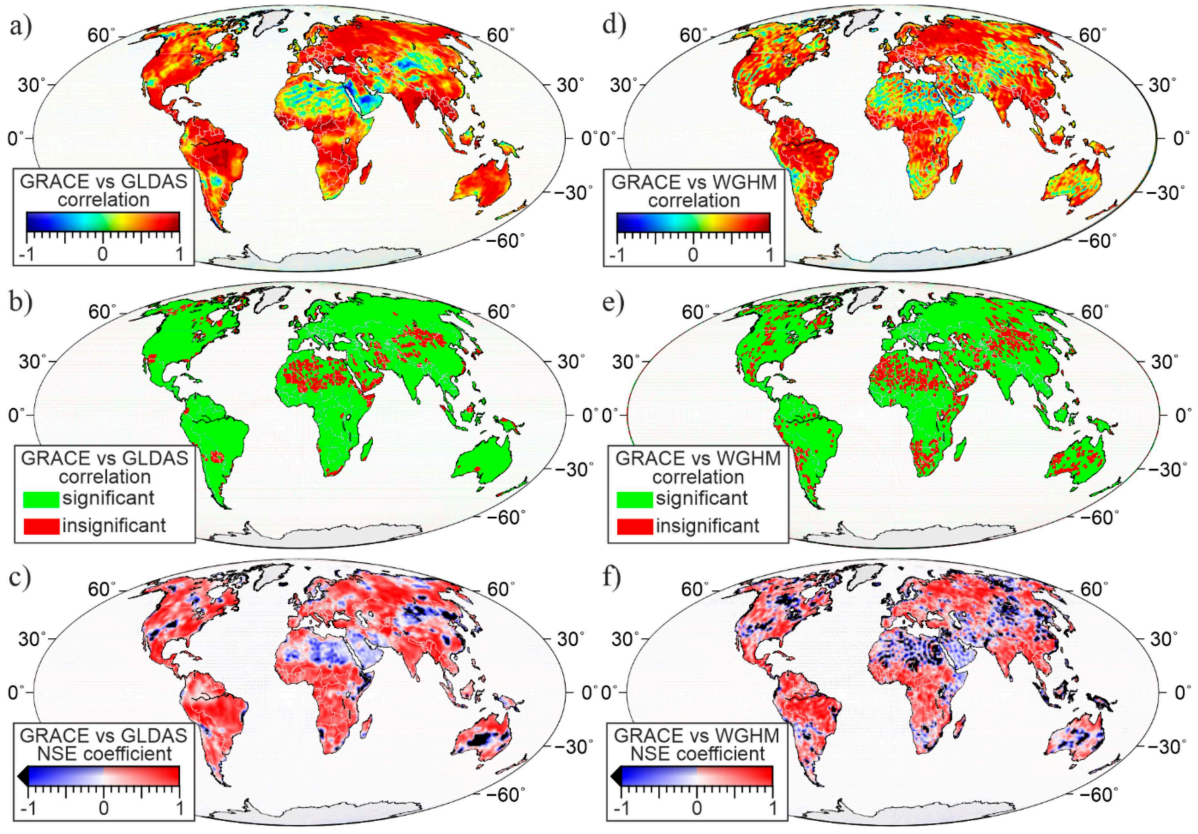

Figure 4. Maps present correlation coefficients, their significance (95% confidence level), and NSE coefficients estimated between TWS changes from GRACE/-FO and TWS changes from hydrological models: GLDAS (**a**–**c**) and WGHM (**d**–**f**), respectively. Estimates are provided for the period of April 2002–December 2019 for both models.

Table 2. Correlation and NSE coefficients estimated for the GRACE/-FO and GLDAS/WGHM hydrological models. Values are unitless.

Statistic Parameter		GRACE/-FO vs. GLDAS	GRACE/-FO vs. WGHM
correlation coefficient	minimum	−0.97	−0.99
	maximum	0.98	0.99
	median	0.21	0.17
	mean	0.20	0.15
NSE coefficient	minimum	−18.7	−176.3
	maximum	0.98	0.99
	median	0.11	0.06
	mean	0.03	−0.28

We find that the TWS differences for the GLDAS and WGHM models are still characterized by trend values of above 2 cm/yr and below −2 cm/yr occurring in the areas of strong groundwater depletion and episodic water changes, such as droughts and floods (central parts of North and South America, and Central and Eastern Asia) (Figure 5a); these constitute regions surrounding the Caspian Sea, the Ganges–Brahmaputra river basin and the Huang He river basin, and areas of the Sao Francisco river basin and Zambezi river basin [2]. The trend values obtained for the TWS differences emphasize the magnitude of underestimating TWS trends within the GLDAS and WGHM hydrological models [9]. Areas of large trend values coincide with the areas of large root mean square (RMS) error, indicating that the RMS of the TWS differences is mainly generated by trends (Figure 5c). Annual amplitudes of TWS differences mainly range between 0 and 25 cm (Figure 5b,e). Values greater than 20 cm for both hydrological models are noted for the Amazon basin. For GLDAS, values up to 5 cm are noted for northern Europe and Asia, and may be caused by seasonal water changes in high latitudes, which are overestimated in the GLDAS hydrological model [44]; this was already presented by [45] for vertical displacements caused by TWS. For WGHM, the amplitude differences are significant additionally for the equator regions (Central Africa, Southern Asia), where we obtained values in the 10–15 cm range. This is caused by underestimating the annual amplitude, especially at low latitudes in the WGHM model [46]. Large trend values and annual amplitudes found for TWS differences for the regions of Alaska and Patagonia may be induced by a missing contribution of glaciers and ice-cap components in the GLDAS and WGHM hydrological models.

The estimated correlation coefficients, the NSE coefficients between the GRACE/-FO and hydrological models, and trends, annual amplitudes, and RMS for the TWS residuals show that the GLDAS and WGHM hydrological models are not able to perfectly reflect the real TWS changes detected by GRACE/-FO for many regions. Consequently, the usage of only a hydrological model to bridge the gap between both GRACE missions may generate uncertainties. Nevertheless, hydrological models are very often employed to assess land hydrology, since they constitute the only high-resolution, continuous, and global dataset to study TWS changes, and they also contain geophysical information. Using analysis-estimated global maps, statistics measures for GRACE/-FO, and both hydrological models, we noted that the GLDAS model was more similar to the GRACE/-FO TWS changes than the WGHM model. This is probably because WGHM tends to overestimate groundwater recharge under semi-arid conditions as in many semi-arid river basins [47]. Furthermore, in contrast to WGHM, the GLDAS model provides data in "near real time" (typically a month's delay). Data from WGHM is made available to users every few years. Thus, if observations from the currently operational GRACE-FO mission are used, the data must be made available as current as possible. Hence, because of the small variety of parameters analyzed in this section, we used the GLDAS model for further study.

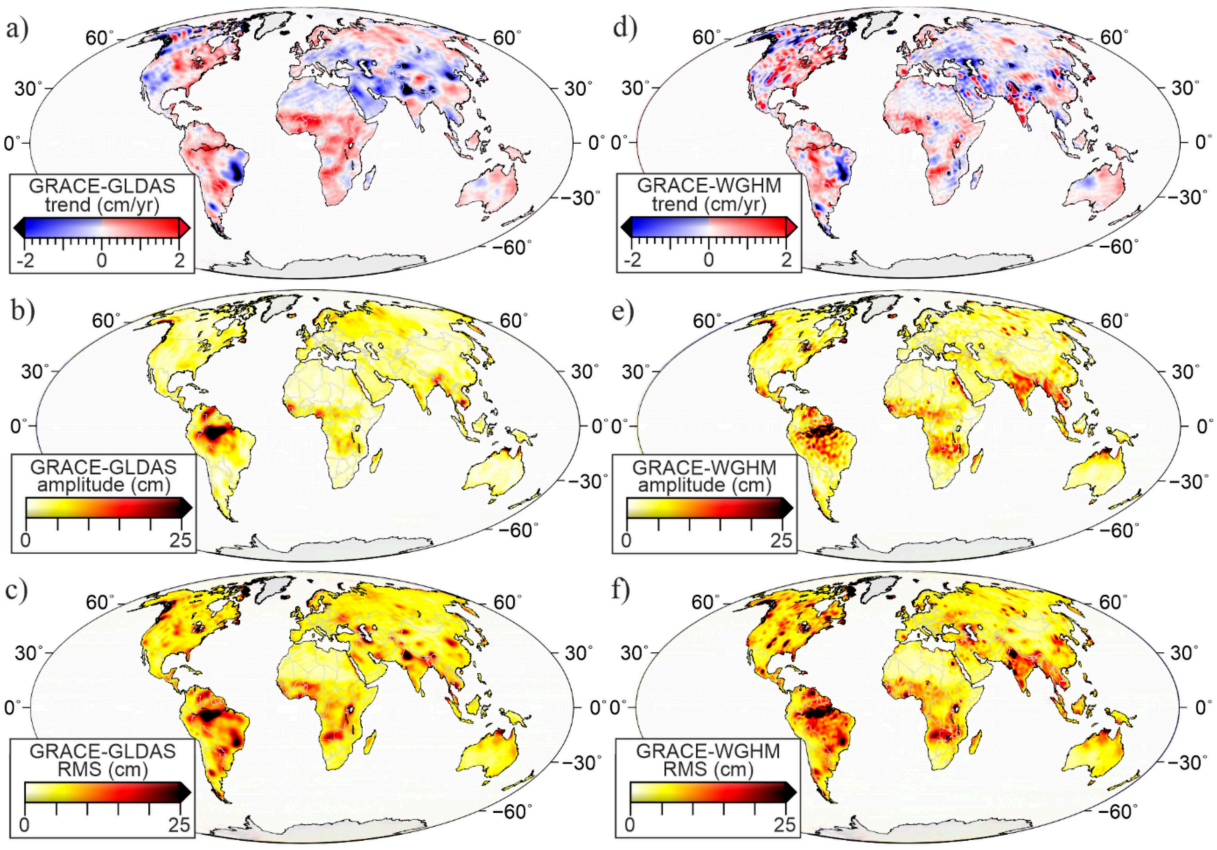

Figure 5. Global maps of linear trends, annual amplitudes, and root mean square error of differences estimated between the GRACE/-FO TWS changes and the (**a**–**c**) GLDAS TWS and (**d**–**f**) WGHM TWS changes for the period of April 2002–December 2019. To estimate trends and annual amplitudes, a simple LSE model is used.

The deterministic model estimated with the LSE algorithm is further removed from the TWS differences to finally end up with the TWS residuals, which are assumed to be stationary, and could, therefore, be subjected to the AR prediction process.

4.3. Test Period: Artificial Gap

To test the AR prediction process, we use continuous GRACE data and create an artificial gap with a period of 11 months, i.e., a time equal to the length of the missing observations between the two GRACE missions. To do that, we choose the mid-GRACE period so that both the forward and backward predictions may be performed. By choosing the mid-GRACE time period, we also omitted the initial months of the GRACE observations and the months after 2010, for which observations were determined with a lower spatial resolution (GRACE Tellus official website). Finally, since the real gap ranged between July 2017 and May 2018, to stay as consistent as possible, we created an artificial gap for the same months, i.e., we chose the period between July 2008 and May 2009.

In Figure 6a, we present the misclosures between the forward- and backward-predicted TWS residuals estimated in the middle of the artificial gap, i.e., in December 2008. The spatial mean value of the global misclosure is equal to 0.09 cm with a median of 2.4 cm, which emphasizes mainly small misclosure values for the whole globe. The largest misclosures occur in areas characterized with rapid TWS changes, which lasted several months before and/or after the artificial gap. For example, misclosures near 13 cm are noticed for the Zambezi river basin, where a decrease in total precipitation was pronounced [48], or for the High Plains Aquifers, where severe droughts led to groundwater pumping [49]. Misclosures close to −13 cm are observed for the Dnieper river basin, characterized by

groundwater decline [2]. To assess the magnitude of misclosures in comparison to the total TWS changes, we estimate the ratio between the misclosures and the difference of the maximum and minimum TWS values, which we hereafter call the "relative error". The relative errors for the time series of global-gridded TWS range between −1.04 (minimum) and 0.83 (maximum). Thus, comparing the relative error values to the total TWS signals in each global node, we showed that the received misclosures are from 3 to 15 times smaller than the total TWS values. For over 60% of global areas, the misclosures' relative errors vary from 0.1 to 0.2 (Figure 6b) with a median equal to 0.02. This means that the misclosures contain only 10–20% TWS signal, and the extreme values of misclosures are covered with regions characterized by maximum values of GRACE annual amplitudes and maximum values of annual amplitude of differences between GRACE and GLDAS (Figure 5b).

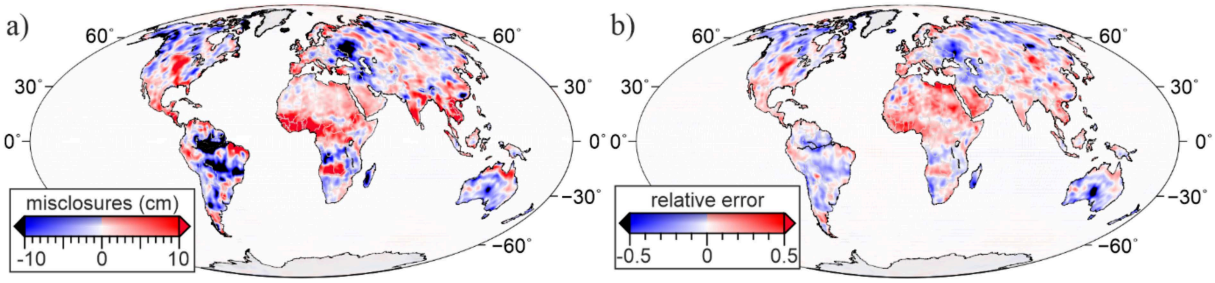

Figure 6. (**a**) Map of misclosures between forward- and backward-predicted TWS residuals, estimated for the mid-gap period, i.e., December 2008. (**b**) Map of the relative error of these, estimated for December 2008.

To compare the results of the hydrological models and to show the validity of using the GLDAS, we also calculated misclosures and their relative error for the WGHM. We obtained a mean value of misclosure equal to 0.37 cm with a median of 2.7 cm. The extreme values of misclosures reach ±15 cm after applying the climatology from the WGHM model. Regions with misclosures above +10 cm and below −10 cm overlap with regions defined from the GLDAS model. However, additional regions appear for the WGHM model in the southern part of North America and in Central Asia.

We focus on a detailed analysis of three areas in which we analyze common signals, computing the averaged time series for all nodes defined in each region. We choose: (1) the Amazon river basin, which is characterized by the largest hydrological changes in the July 2008 to May 2009 period [50], (2) the Northern Territory of Australia, which is characterized by significant inter-annual variations of TWS in the July 2008 to May 2009 period [28], and (3) a region of Central Europe, which is often presented as the one with insignificant hydrological changes [2]. The area of the Northern Territory of Australia is defined after [51]. Central Europe is defined according to [52].

The comparison of time series between the TWS residuals and their prediction for the artificially generated gap shows that predicted values agree well with the TWS residuals (Figure 7). The predicted TWS residuals for the Amazon river basin are very close to the TWS residuals (compare the blue, red, and gray lines in Figure 7a). The forward prediction follows the TWS residuals, while the backward prediction traces decreasing values nicely. The forward and backward predictions do not meet with each other. The misclosure is equal to 4 cm; its relative error equals 0.05. In this case, half of the misclosure, i.e., 2 cm, is scattered for the forward- and backward-predicted time series to obtain continuous changes of the predicted TWS residuals within the artificial gap. The bridged time series (red line in Figure 7a) almost identically coincides with the real nature of the TWS residuals (grey line). The predicted TWS residuals for the Northern Territory of Australia (Figure 7b) and Central Europe (Figure 7c) are also characterized by a good agreement with the TWS residuals. Misclosures are equal to, respectively, 0.3 cm and 0.2 cm, with relative errors equal to, respectively, 0.06 and −0.04. For both regions, the misclosures are equal to a few millimeters, so the bridged time series of the predicted TWS residuals (red lines in

Figure 7b,c) and the predicted TWS residuals obtained for the forward and backward predictions (blue lines in Figure 7b,c) overlap. For Europe (Figure 7c), the changes in the predicted TWS residuals for the first months of the gap are underestimated, which is probably caused by the length of occurred drought before the prediction period (orange stripes in Figure 7c). The results show that the presented method is able to reflect the monthly TWS changes in the time series, especially in regions characterized by small hydrological variations.

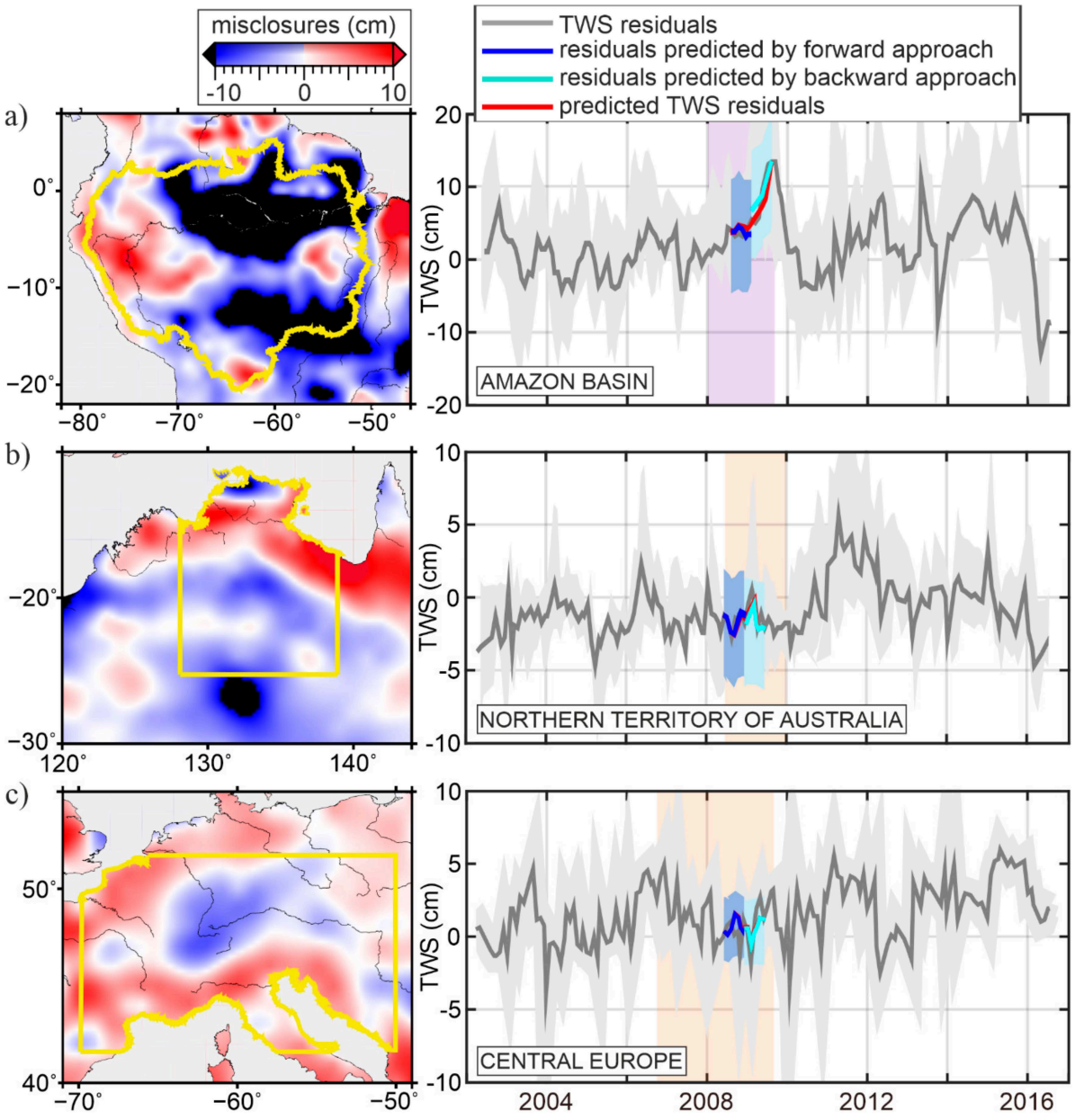

Figure 7. AR prediction of TWS residuals presented for (**a**) the Amazon river basin, (**b**) the Northern Territory of Australia, and (**c**) Central Europe. Prediction is performed for the artificial gap period of July 2008 to May 2009. Individual regions are presented on maps in the right column, where the background color presents the values of misclosures between forward and backward predictions of the TWS residuals. Plots in the left column represent the TWS residuals, along with their prediction for the artificial gap. The shaded areas define the spatial variation of the TWS residuals for individual regions, while the colored stripes define wet (in violet) and dry (in orange) periods.

We add the LSE deterministic signal and GLDAS TWS changes back to the predicted TWS residuals and estimate the predicted GRACE TWS changes for global nodes in $1^\circ \times 1^\circ$ grid. We compare the predicted GRACE TWS values with the GRACE TWS for the artificial gap, from July 2008 to May 2009. We estimate the sum of differences between the GRACE TWS and the predicted GRACE TWS. We find the maximum value for the equatorial areas and Northern Asia regions (Figure 8a), for which the sum of differences varied by $\pm$150 cm for all 11 months of the artificial gap. These areas coincide with the regions characterized by the largest annual amplitude computed between the GRACE TWS and GLDAS TWS differences. Thus, the values in Figure 8a also prove that the AR predictions are not efficient enough for regions where GLDAS underestimates real hydrological changes. We also note that TWS differences may still contain signals in inter-annual and sub-seasonal period bands, which means that the prediction process may be less efficient for these regions; not all TWS components are modeled within the GLDAS hydrological model, e.g., missing surface water or groundwater components. Consequently, for, i.e., Amazon, Alaska, and the south part of Asia regions, the absolute values of the sum of differences between the GRACE TWS and the GLDAS TWS (the "TWS differences") are between 200 cm and 350 cm. This means that our method predicts the GRACE TWS changes better than the standalone GLDAS hydrological model by at least 25% for these areas.

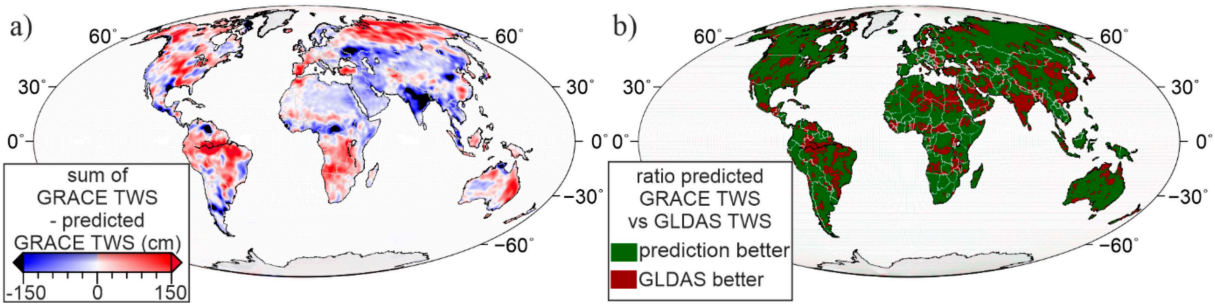

Figure 8. (**a**) Global sum of differences estimated between the GRACE TWS changes and the predicted GRACE TWS changes. (**b**) Global map of the ratio estimated between (1) the GRACE TWS changes minus the predicted GRACE TWS changes and (2) the GRACE TWS changes minus the GLDAS TWS changes; see Equation (7). The green color means that AR prediction works better than the standalone GLDAS TWS changes to fill the gap, while the red color means that GLDAS is better than the AR prediction. Values in (**a**,**b**) are computed for the artificial gap period, from July 2008 to May 2009.

The essential impact of the GLDAS model on the results presented in Figure 8a and on the predicted TWS times series is confirmed by the sum of difference values calculated between the original TWS residuals and the predicted TWS residuals for the artificial gap period (July 2008–May 2009). We obtained values ranging from -63 cm to 56 cm for all global grid nodes. The spatial mean value for continental areas is equal to -18.3 cm with a median equal to -21.2 cm. Extreme values were obtained for the Amazon basin, Patagonia, India, and Northern Asia regions. The received numbers show the credibility of the proposed two-step approach, i.e., removing climatology using both GLDAS and LSE before the prediction process. In this way, we remove the "imperfections" of the GLDAS model (underestimation of changes observed by GRACE) and the "imperfections" of the LSE method (does not contain geophysical effects in the LSE model).

We also evaluated the global comparison of the predicted GRACE TWS estimated by the GLDAS model using the gridded GRACE-REC dataset. As for the predicted GRACE TWS (Figure 8a), we compared the original GRACE TWS values in the artificial gap with those from GRACE-REC, calculating the sum of their differences. GRACE-REC is a global reconstruction of the total TWS changes that was developed from: (1) GSFC and JPL GRACE mascons, and (2) historical and near-real-time meteorological datasets. They are made available to users by [17]. Similar to our approach, in the case of GRACE-REC, we obtained maximum values for the sum of differences at 90 cm in the Amazon region. Values greater

than 50 cm were also obtained in the southern part of Africa and the central part of North America, such as for our methodology. In contrast, values of the sum of differences below −50 cm are covered with the Patagonia area and the Western Europe/Eastern Asia, Central Asia, and Western Australia regions. We received larger values for the sum of differences for our method in the regions of northern and southern Asia, which are, respectively, due to the overestimation of precipitation and the lack of modeling anthropogenic impacts (irrigation process) in the GLDAS hydrological model.

We also evaluated the regional comparison of our results with GRACE-REC and the datasets provided by [22,53]. The data provided by [22] are predicted GRACE-like gridded TWS changes available for 26 river basins, oceans, and seas, which were reconstructed using CSR GRACE mascons and climate inputs. Both [22,53] used, among others, precipitation, land temperature, sea surface temperature, evaporation, surface runoff, and climate indices as inputs to the reconstruction process. Ref. [53] provides reconstructed TWSA fields by combining machine learning with time series decomposition and statistical decomposition techniques. In Table 3, we present a few statistics estimated for time series in the artificially generated gap. A comparison with [22] was made only for two of our regions—Amazon river basin and Central Europe, which cover the Amazon and Ob river basins, respectively.

Table 3. Comparison of average time series for selected regions obtained as difference between (1) the original GRACE TWS and the predicted GRACE TWS values based on the GLDAS model (our method), and (2) the original GRACE TWS and the previous study. Values in centimeters.

Selected Region	Measure Statistics	Our Method	Ref. [17]	Ref. [22]	Ref. [53]
Amazon river basin	median	−1.8	1.0	−0.8	3.4
	RMS	6.3	3.2	5.5	6.7
	sum	44.6	28.2	22.8	33.1
Northern Territory of Australia	median	0.6	0.7	-	−2.3
	RMS	0.5	2.8	-	4.1
	sum	5.0	−6.3	-	7.6
Central Europe	median	0.7	1.1	1.7	1.1
	RMS	0.3	1.2	2.1	3.8
	sum	8.1	2.2	7.3	7.5

The results presented in Table 3 emphasized that our proposed method gives comparable results with other approaches. Our method is even better in the case of the Australian and European regions. Median values are of the same order for the Central Europe region, and the RMS is several times smaller for our approach than for others (excluding the Amazon region). The divergences in the Amazon region are probably caused by using the GLDAS as climatology, which mis-models the TWS in this area. In the Amazon region, we also obtained the large difference in annual amplitude (Figure 5b) and RMS (Figure 5c) parameters between GRACE and GLDAS. This was probably caused by the occurrence of the greatest RMS values for the GRACE data in the Amazon basin, and by mis-modeling the surface water and groundwater components in the GLDAS model, which are essential in the Amazon region. Consequently, we obtained nearly twice-greater sum values and the largest RMS of all methods. The lowest median and RMS values in the European and Australian regions for our results are probably due to the dominant influence of the soil moisture component in both cases, which is well modeled by GLDAS [33]. The results show that our approach is better or comparable to other methods for regions where climatology (GLDAS) contains the main TWS components.

Furthermore, to assess the quality of the AR prediction method for gap filling, we use the GRACE TWS changes and the GLDAS TWS changes, along with the predicted GRACE TWS values, and estimate the ratio (R_{TWS}):

$$R_{TWS} = \left| \frac{\text{GRACE TWS} - \text{predicted GRACE TWS}}{\text{GRACE TWS} - \text{GLDAS TWS}} \right| \quad (9)$$

A ratio smaller than 1 means that the AR prediction works better than the standalone GLDAS hydrological model to fill the GRACE gap. A ratio greater than 1 means that the GLDAS hydrological model is efficient enough to fill the GRACE gap and works better than AR prediction (Figure 8b). From Figure 8b, we notice that the AR prediction reflects the TWS changes observed by GRACE better than the standalone GLDAS hydrological model for more than 75% of regions.

It can be noticed that the areas marked in brown (i.e., regions of South America, Southern and Central Asia, and Northern Europe and Africa) in Figure 8b coincide with the places of low correlation between the GRACE TWS changes and GLDAS TWS changes (Figure 3a). This is related to a disagreement of trend values (Figure 4a) in South America and Southern Asia, and to a disagreement of annual amplitudes (Figure 4b) in Northern Europe and Asia. Moreover, most regions marked in brown coincide with the RMS of GRACE–GLDAS differences, for which the values are greater than 20 cm (Figure 4c). The obtained results emphasize that AR prediction reflects the predicted TWS time series better than the GLDAS hydrological model for regions characterized by small hydrological seasonal signals. This is confirmed by absolute values of a ratio greater than 1 for, i.e., the Amazon, Eastern Europe, or Northern Australia areas, where the RMS is maximum (Figure 4c). On the other hand, the regional analysis of the predicted TWS monthly values (Figure 7) shows that the values presented in Figure 8 are influenced mainly by the magnitude of differences for individual months calculated between the GRACE TWS changes and the predicted GRACE TWS changes during the artificial gap.

To assess the quality of the reconstructed signals, we estimate the latitude-weighted MAE (Equation (7)) and the latitude-weighted RMSE (Equation (8)) of the differences between the GRACE TWS and the predicted GRACE TWS changes for the artificial gap. Both parameters were estimated for the selected regions, e.g., the Amazon, the Northern Territory of Australia, and Central Europe. To estimate the MAE and RMSE values for individual months, we divide the obtained errors in Equations (7) and (8) by 11 (the number of months during the gap). As a result, the MAE and RMSE values are presented in Table 4. Globally, the MAE and RMSE are equal to 3.3 cm and 5.1 cm, respectively, which is similar to the values of error of the GRACE/-FO gap filling estimated by [28] using the iteration MSSA approach, i.e., 4.1 cm and 5.8 cm.

Table 4. Latitude-weighted MAE and RMSE parameters estimated for regional analysis. Values in centimeters/month.

	MAE	**RMSE**
Amazon basin	1.5	2.8
Northern Territory of Australia	3.1	7.5
Central Europe	1.7	5.0

Our approach is different from the forward-only prediction presented by previous studies [23]. Our global analysis of forward-only and forward–backward-predicted values showed that for the forward-only approach, the magnitude of misclosures is greater by 3 times on average than the magnitudes of misclosures estimated for forward–backward prediction. For the forward-only approach, misclosures are estimated as the difference between last values of the predicted TWS residual time series and the TWS residual values for the first month of the GRACE-FO data. The largest discrepancies in misclosures between the forward-only and forward–backward predictions, from 10 to 22 cm, occur in areas

characterized by significant TWS trends, around ±2 cm/yr. These are Eastern Brazil, Alaska, Northwestern Australia, the Caspian and Aral Seas, Southwestern Russia, and the North China Plain. This shows that the forward–backward approach is able to predict the future rate of TWS changes more reliably than the forward-only approach. A comparison between the GRACE TWS and the predicted GRACE TWS changes for the forward-only and forward–backward predictions shows that the forward-only predicted GRACE TWS changes are on average 1.6-times greater than the forward–backward-predicted GRACE TWS changes, with a median equal to 1.2. The greatest divergences between both prediction approaches occurs in regions with the largest hydrological changes, i.e., Central Brazil, Central Africa, the Ganges–Brahmaputra river basin, and the Northern Russia region. In these areas, we obtain the sum of difference discrepancies between both approaches, even up to 60 cm.

4.4. Filling the Real GRACE/-FO Gap

We analyze the ability of the AR process to fill the natural gap between the GRACE and GRACE-FO missions, i.e., the period from July 2017 to May 2018. Figure 9 presents the misclosures estimated between the forward- and backward-predicted TWS residuals for the mid-gap month, i.e., December 2017, along with their relative errors.

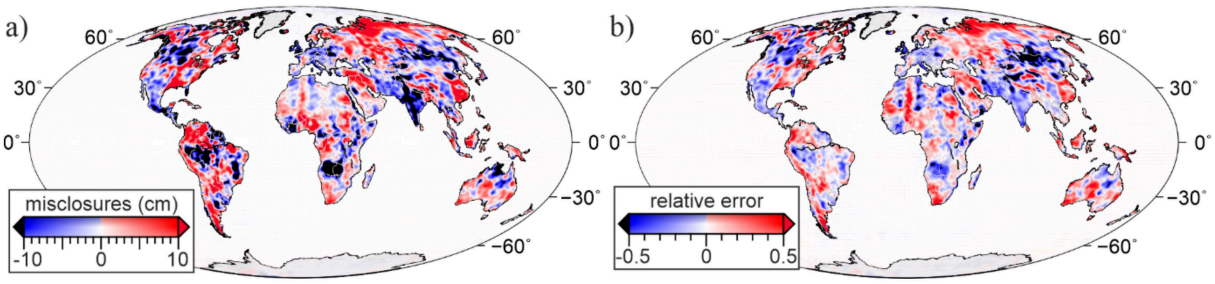

Figure 9. Maps of (**a**) misclosures estimated between forward- and backward-predicted TWS residuals and (**b**) their relative error. Estimates are provided for the mid-gap month, i.e., December 2017.

Figure 9a shows that for over 70% of continental areas, misclosures between the forward- and backward-predicted TWS residuals are below 10 cm and above −10 cm. The extreme values occur around the 20°–30° parallels in both hemispheres and in regions around the North Arctic Circle (Northern Canada and Eurasia regions). These areas coincide with regions of strong influence of El Niño and La Niña phenomena [54] and increasing precipitation [2]. Regions recognized as those with large episodic water phenomena during the natural gap are characterized by misclosures greater than ±10 cm. For example, maximum misclosures equal to 12 cm in the High Plains Aquifer region result from rapid floods in early 2017 and heavy rainfall in 2019 [3]. The minimum misclosures equal to −13 cm occurring in South Africa may be caused by floods noted for the last months of the GRACE mission and the first months of the GRACE-FO mission. Analyzing the relative error of misclosures of the TWS residuals (Figure 9b), we acknowledge that the obtained misclosures respond to at least 20% of the total signal of land hydrology in 80% of areas. The largest relative error (over 50%) occurs in the Western, Central, and Northern Asia regions. In the western and central parts of the continent, this may be explained by strong groundwater depletion [2], since the GLDAS hydrological model has natural groundwater cycles excluded. In the Northern Russian regions, it results from large differences of annual amplitude (around 10 cm. Figure 4b) between the GRACE/-FO and GLDAS, which is caused by an overestimation in precipitation in the land surface model [44].

Next, we present the time series of the predicted TWS residuals for the natural gap between both GRACE missions for the same regions, as discussed in the previous section and presented in Figure 7. Misclosures estimated between forward- and backward-predicted TWS residuals are equal to 2.5 cm, −4.8 cm, and −2.3 cm with relative errors equal to 0.05, −0.08, and −0.16, for, respectively, the Amazon river basin, the Northern Territory of

Australia, and Central Europe. To obtain a continuous signal in land hydrology, misclosures are removed by scattering proportionally for time series estimated for both the forward and backward approach, separately. The results are then presented in Figure 10. Furthermore, to assess the monthly TWS changes in detail, we mark wet (heavy rainfall and floods) and dry (increase of average temperature and emerging droughts) periods which occurred in the chosen regions in Figure 10. These are represented by the violet and orange background colors, respectively. The first region, the Amazon river basin, is a specific area characterized by an alternating number of floods and droughts during the operation of GRACE/-FO, i.e., the period from 2002–2021. In the Amazon region, for the last months of the GRACE mission and during the first months of the natural gap, a decrease in water was noticed (Figure 10a). These periods agree very well with the drought that occurred in 2017, which was also observed by the Swarm mission [11]. Similar continental water changes occur in Australia (Figure 10b) and Europe (Figure 10c). In the Northern Territory of Australia, droughts occurred from the end of 2017 onwards (decreasing rainfall; Technical Note Water in Australia 2017–2018). Consequently, a loss in water storage is noticeable in Figure 10b. On the other hand, according to the Australian Bureau of Meteorology, the first months of 2018 were characterized by an increasing sum of precipitation. That phenomena reflects the 1.3 cm increase in the TWS residuals values noticed in Figure 10b. In the case of Central Europe, there were also a few severe drought periods, i.e., from July 2016 to June 2017 [55], from spring 2018 onwards (Earth Observatory website; [56]) and in 2019–2020 [57]. This is observed as water loss in the TWS residuals and the predicted TWS residuals (Figure 10c), which reflect the TWS values declining, especially at the turn of 2017/2018.

We now restore the LSE deterministic signals (trend and seasonal oscillations), and the climatology from the GLDAS hydrological model, back to the predicted TWS residuals. We obtain the predicted GRACE/-FO TWS values presented in Figure 11 (blue and red curves). Similar to the residuals (Figure 10), in Figure 11, we also mark wet (violet background) and dry (orange background) periods. For the Amazon river basin and Central Europe regions, a significant annual curve over the real gap is noticeable, whereas for all regions, a TWS decrease is captured in the first months of the natural gap period (drought events). To assess the quality of the obtained TWS changes for the gap period, we determine the TWS changes from the Swarm mission (yellow curve). Although the Swarm product is up to 40 degrees, we only compared degrees up to 12. The obtained monthly changes for the Amazon region (Figure 11a) coincide with the TWS changes from the Swarm data, but the magnitude of seasonal changes is mainly underestimated, especially during the GRACE-FO period. The Swarm's underestimation of TWS changes observed by GRACE for the Amazon region has been shown previously by [7,11]. However, the determined TWS time series from Swarm confirm the reliability of the obtained changes. For both cases, there is an apparent decrease in TWS values in the first months of the gap, an increase in the following months, and another decrease after 2018 (Figure 11a). The TWS changes for the Amazon area were also analyzed by combined gravity data [58], and the TWS changes were estimated by the stochastic approach, i.e., the singular spectrum analysis (SSA, [23] or MSSA [59]) methods, in which authors noted similar variations of monthly TWS changes. For Australia, the monthly TWS changes determined by Swarm overestimate the GRACE/-FO TWS and predicted GRACE TWS values (Figure 11b). The Swarm TWS time series are characterized by more frequent monthly variations than the GRACE/-FO TWS. Although, for both the Swarm TWS and the predicted GRACE/-FO TWS time series, a generally similar seasonality of monthly changes is noticed, i.e., a decrease, increase, and decrease in TWS values. For Australia, filling the natural gap using the Swarm mission observations has been already shown by [7], where the TWS loss was emphasized (drought period) in the north part of the continent. It is noted by a 15 cm TWS decrease from Swarm in the last months of 2017 (Figure 11b), which reflects 10 cm and 2 cm changes in the predicted GRACE/-FO TWS (Figure 11b) and TWS residual (Figure 10b) time series, respectively. In the case of the Central Europe region, the monthly GRACE/-FO TWS and predicted GRACE/-FO TWS are overestimated by the Swarm TWS, but the general seasonality of the TWS changes is

similar. Both the Swarm TWS and the predicted GRACE/-FO TWS catch a decrease and an increase in the TWS values in the first and second half of the real gap period, respectively. However, for the Swarm TWS time series, we can see an about 5 cm increase in TWS values around July/August 2017, which is probably due to the spatial resolution of the Swarm missions (equal to 3000–4000 km) and/or the truncation of the spherical harmonics to a low degree. The decline in continental water storage in first month of 2018 for the Danube river basin was also marked by [11], which is reflected by a TWS decrease equal to 13 cm (Figure 11c) and TWS residual changes equal to 2 cm (Figure 10c). However, Ref. [23] presented 13 cm of TWS loss for the seasonal autoregressive integrated moving average (SARIMA) and SSA methods. They estimated the TWS variability in the natural gap for the Amazon area. Presented in Figure 11a, the monthly TWS changes are characterized by a good agreement with stochastic models in the natural gap period. For example, we noticed a 35 cm TWS increase for the predicted GRACE/-FO TWS in 2017/2018 (Figure 11a), similar to [23]. The described regional analyses show that the presented prediction method can be also used effectively to study the seasonal and episodic changes in terrestrial water storage time series, among others, for missing data in hydrological models or Swarm mission observations, which often under- or overestimate the regional TWS changes observed by GRACE/-FO.

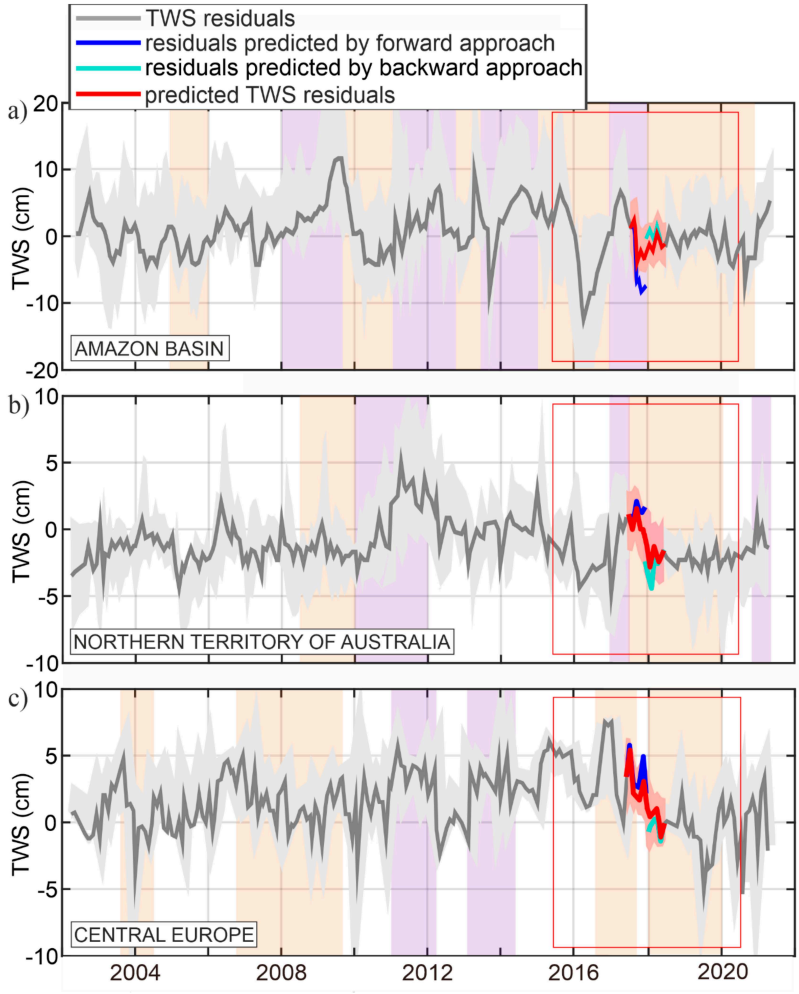

Figure 10. TWS time series of predicted TWS residuals for the (**a**) Amazon river basin, (**b**) Northern Territory of Australia, and (**c**) Central Europe regions for the natural gap (July 2017 to May 2018). The shaded time series areas define the spatial variation of the signal, and the color stripes define wet (violet) and dry (orange) periods that occurred in the selected areas. The red rectangle shows the months used in the forecasting process.

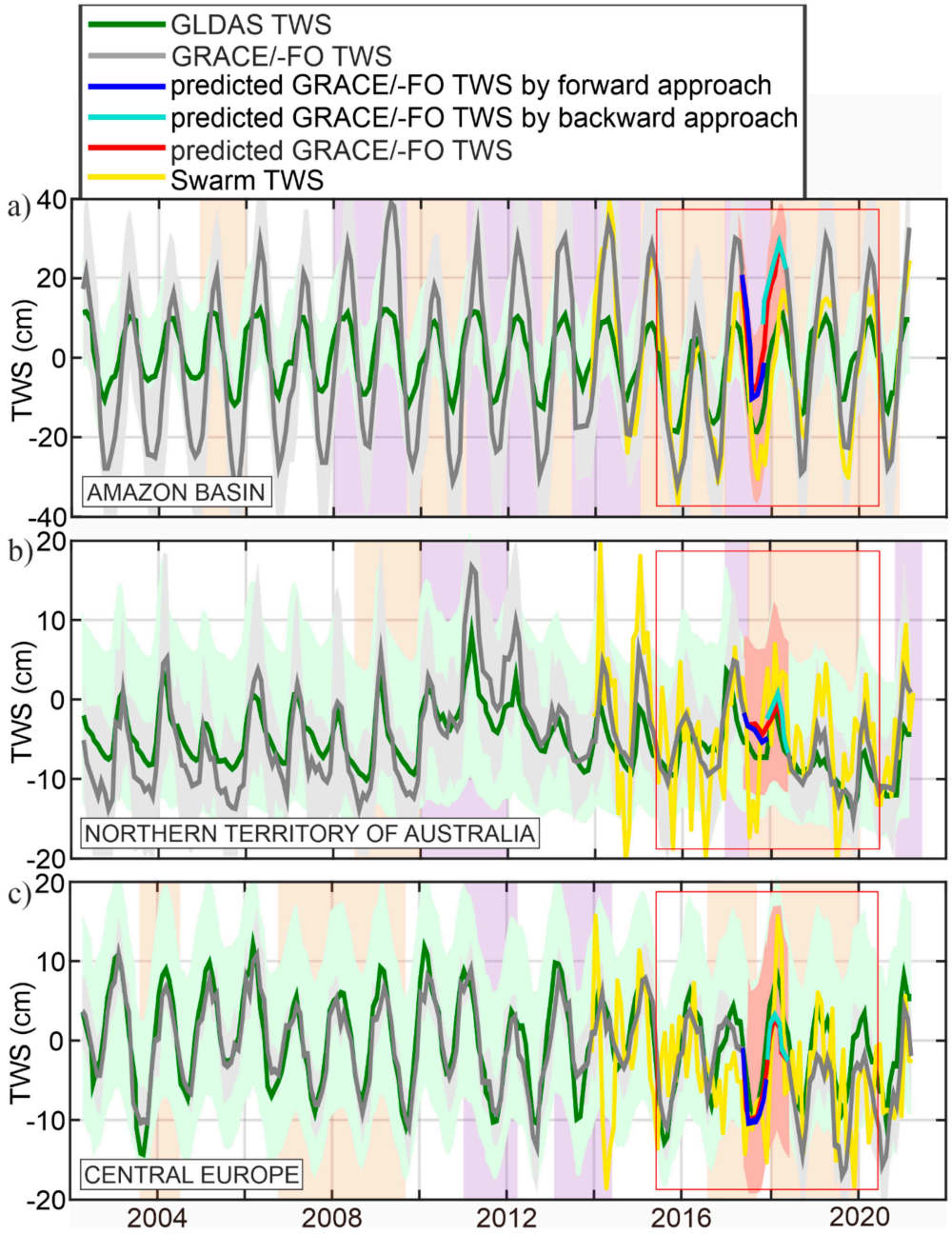

Figure 11. Time series of predicted GRACE/-FO TWS values for the (**a**) Amazon, (**b**) Northern Territory of Australia, and (**c**) Central Europe regions for the generated artificial gap (July 2017 to May 2018). The shaded time series areas define the spatial variation of the signal, and the color stripes define wet (violet) and dry (orange) periods that occurred in the selected areas.

5. Summary and Conclusions

Water availability is changing worldwide as a result of human activity and climate change impact, which now has been successfully observed by the GRACE/-FO missions. These changes are driven by, among other things, unsustainable groundwater consumption, climate change, interannual natural variability, or a combination thereof. In many regions, these drivers cause significant long-term changes, non-linear short-term changes, and significant seasonal annual and semi-annuals changes which ultimately concur to GRACE climatology. The estimation of this natural inter-annual variability of the TWS anomaly is possible by, among other things, using global hydrological models, i.e., GLDAS or the WGHM hydrological model.

We present a new approach to bridge the observation of TWS changes between the GRACE and GRACE-FO missions. Our process of forecasting 11 months' worth of missing TWS changes is based on the remove–restore technique using AR backward and forward prediction and hydrological models. Based on the autocovariance function estimated separately for GRACE and GRACE-FO data, we adopt the length of 24 months as optimal for both the forward and backward approaches to estimate the coefficients of the autoregressive model. The prediction was based on the TWS residuals, which we obtained after removing climatology and deterministic signals (i.e., trend, annual, and semiannual oscillations) from the GRACE/-FO TWS. We defined climatology using the GLDAS and WGMH hydrological models. Finally, due to, among other things, "near-real-time" GLDAS data availability and a small variety of parameters, we used the GLDAS model for further analysis. To assess the quality of the proposed method, we tested it for an artificially generated gap during the GRACE mission operation (the period from July 2008 to May 2009). The obtained global sum of residuals estimated between the original GRACE TWS and the predicted GRACE TWS changes shows that our prediction process is not efficient enough for regions where the GLDAS hydrological model underestimates real geophysical changes; mis-modeled TWS compartments are still present in the residuals which undergo the prediction process. The regional analysis performed for the Amazon river basin, the Northern Territory of Australia, and Central Europe shows that the predicted TWS residuals are characterized by a good agreement with the monthly TWS residuals (Figure 7). It is shown that the AR model can be well fitted to irregular total water storage residuals and is able to capture the occurrence of dry and wet periods. However, this result holds for certain geographic locations only, including some parts of the equator. The credibility of the presented approach is assessed based on the latitude weighted mean absolute error and the latitude weighted root mean square error, which are estimated between the GRACE TWS and the predicted GRACE TWS changes for the artificial gap. The obtained global values are equal to 3.3 cm and to 5.1 cm for, respectively, the MAE and RMSE. The obtained values emphasize a high compliance with other stochastic methods used for GRACE/-FO gap filling, such as the iteration MSSA approach. In the case of the natural gap, we obtain maximum values of TWS misclosures for regions where strong El Niño and La Niña phenomena occurred. Moreover, we notice that for the real gap, the AR misclosures represent at least 20% of the total land hydrology signal for 80% of the areas. The greatest values of the misclosures' relative error are obtained for the Western and Central Asia regions, where a strong groundwater depletion appears. We show that the remove–restore technique allows for filling the GRACE/-FO gap more reliably than the standalone GLDAS hydrological model for more than 75% of continental regions (Figure 8b). However, since the proposed prediction approach is based on the GLDAS hydrological model, we can predict TWS changes much more reliably for regions characterized with insignificant seasonal hydrological effects. So, our method may be more efficient if other hydrological models are employed, especially those well-correlated with real changes for individual regions. It should be mentioned that the proposed method still provides new opportunities for filling the GRACE/-FO gap next to the other approaches and can be a viable alternative to fill in not only GRACE-type data, but other types as well.

Author Contributions: Conceptualization: A.L., M.W. and W.K. Manuscript preparation: A.L., M.W., W.K. and J.M. Methodology and data analysis: A.L., W.K., M.W. and J.M. Discussion: A.L., M.W. and W.K. Figure preparation: A.L. and J.M. All authors have read and agreed to the published version of the manuscript.

Funding: This research was financed by the funds granted to A.L. for Young Scientists' support by the Faculty of Civil Engineering and Geodesy, Military University of Technology, Poland. Grant number 1/WSFN/2020.

Institutional Review Board Statement: Not applicable.

Informed Consent Statement: Not applicable.

Data Availability Statement: The CSR mascon solutions are available on the http://www2.csr.utexas.edu/grace/RL06_mascons.html website (accessed on 1 July 2021); the GLDAS Noah hydrology loading model is available on the https://disc.gsfc.nasa.gov/datasets/GLDAS_NOAH10_M_2.1/summary?keywords=GLDAS%20noah website (accessed on 1 July 2021).

Acknowledgments: We are grateful to CSR for providing GRACE Level-2 observations in the form of a mascon solution, and to Goddard Earth Sciences Data and Information Services Center (GES DISC) for providing GLDAS Noah hydrology loading model. More information about the GRACE and GRACE-FO missions can be found at https://gracefo.jpl.nasa.gov (accessed on 1 July 2021) and at https://www.gfz-potsdam.de/en/grace-fo (accessed on 1 July 2021), respectively. Maps were drawn in the Generic Mapping Tools software [60].

Conflicts of Interest: The authors declare no conflict of interest.

References

1. Tapley, B.D.; Bettadpur, S.; Watkins, M.; Reigber, C. The gravity recovery and climate experiment: Mission overview and early results. *Geophys. Res. Lett.* **2004**, *31*, L09607. [CrossRef]
2. Rodell, M.; Famiglietti, J.S.; Wiese, D.N.; Reager, J.T.; Beaudoing, H.K.; Landerer, F.W.; Lo, M.-H. Emerging trends in global freshwater availability. *Nature* **2018**, *557*, 651–659. [CrossRef] [PubMed]
3. Landerer, F.W.; Flechtner, F.M.; Save, H.; Webb, F.H.; Bandikova, T.; Bertiger, W.I.; Bettadpur, S.V.; Byun, S.H.; Dahle, C.; Dobslaw, H.; et al. Extending the Global Mass Change Data Record: GRACE Follow-On Instrument and Science Data Performance. *Geophys. Res. Lett.* **2020**, *47*, e2020GL088306. [CrossRef]
4. Richter, H.M.P.; Lück, C.; Klos, A.; Sideris, M.G.; Rangelova, E.; Kusche, J. Reconstructing GRACE-type time-variable gravity from the Swarm satellites. *Sci. Rep.* **2021**, *11*, 1117. [CrossRef]
5. Weigelt, M.; van Dam, T.; Jäggi, A.; Prange, L.; Tourian, M.J.; Keller, W.; Sneeuw, N. Time-variable gravity signal in Greenland revealed by high-low satellite-to-satellite tracking. *J. Geophys. Res. Solid Earth* **2013**, *118*, 3848–3859. [CrossRef]
6. Ferreira, V.G.; Ndehedehe, C.E.; Montecino, H.C.; Yong, B.; Yuan, P.; Abdalla, A.; Mohammed, A.S. Prospects for Imaging Terrestrial Water Storage in South America Using Daily GPS Observations. *Remote Sens.* **2019**, *11*, 679. [CrossRef]
7. De Encarnação, J.T.; Visser, P.; Arnold, D.; Bezdek, A.; Doornbos, E.; Ellmer, M.; Guo, J.; van den Ijssel, J.; Iorfida, E.; Jäggi, A.; et al. Multi-approach gravity field models from Swarm GPS data. *Earth Syst. Sci. Data* **2019**, *12*, 1–55. [CrossRef]
8. Soltani, S.S.; Ataie-Ashtiani, B.; Simmons, C.T. Review of assimilating GRACE terrestrial water storage data into hydrological models: Advances, challenges and opportunities. *Earth-Science Rev.* **2020**, *213*, 103487. [CrossRef]
9. Scanlon, B.R.; Zhang, Z.; Save, H.; Sun, A.Y.; Schmied, H.M.; van Beek, L.P.H.; Wiese, D.N.; Wada, Y.; Long, D.; Reedy, R.C.; et al. Global models underestimate large decadal declining and rising water storage trends relative to GRACE satellite data. *Proc. Natl. Acad. Sci. USA* **2018**, *115*, E1080–E1089. [CrossRef]
10. Meyer, U.; Sosnica, K.; Arnold, D.; Dahle, C.; Thaller, D.; Dach, R.; Jäggi, A. SLR, GRACE and Swarm Gravity Field Determination and Combination. *Remote Sens.* **2019**, *11*, 956. [CrossRef]
11. Forootan, E.; Schumacher, M.; Mehrnegar, N.; Bezděk, A.; Talpe, M.J.; Farzaneh, S.; Zhang, C.; Zhang, Y.; Shum, C.K. An Iterative ICA-Based Reconstruction Method to Produce Consistent Time-Variable Total Water Storage Fields Using GRACE and Swarm Satellite Data. *Remote Sens.* **2020**, *12*, 1639. [CrossRef]
12. Zhang, X.; Li, J.; Dong, Q.; Wang, Z.; Zhang, H.; Liu, X. Bridging the gap between GRACE and GRACE-FO using a hydrological model. *Sci. Total Environ.* **2022**, *822*, 153659. [CrossRef]
13. Rahaman, M.M.; Thakur, B.; Kalra, A.; Ahmad, S. Modeling of GRACE-Derived Groundwater Information in the Colorado River Basin. *Hydrology* **2019**, *6*, 19. [CrossRef]
14. Forootan, E.; Kusche, J.; Loth, I.; Schuh, W.-D.; Eicker, A.; Awange, J.; Longuevergne, L.; Diekkrüger, B.; Schmidt, M.; Shum, C.K. Multivariate prediction of total water storage anomalies over West Africa from multi-satellite data. *Surv. Geophys.* **2014**, *35*, 913–940. [CrossRef]
15. Mo, S.; Zhong, Y.; Forootan, E.; Mehrnegar, N.; Yin, X.; Wu, J.; Feng, W.; Shi, X. Bayesian convolutional neural networks for predicting the terrestrial water storage anomalies during GRACE and GRACE-FO gap. *J. Hydrol.* **2021**, *604*, 127244. [CrossRef]
16. Löcher, A.; Kusche, J. A hybrid approach for recovering high-resolution temporal gravity fields from satellite laser ranging. *J. Geod.* **2020**, *95*, 6. [CrossRef]
17. Humphrey, V.; Gudmundsson, L. GRACE-REC: A reconstruction of climate-driven water storage changes over the last century. *Earth Syst. Sci. Data* **2019**, *11*, 1153–1170. [CrossRef]
18. Yi, S.; Sneeuw, N. Filling the Data Gaps within GRACE Missions Using Singular Spectrum Analysis. *J. Geophys. Res. Solid Earth* **2021**, *126*, e2020JB021227. [CrossRef]
19. Gyawali, B.; Ahmed, M.; Murgulet, D.; Wiese, D.N. Filling Temporal Gaps within and between GRACE and GRACE-FO Terrestrial Water Storage Records: An Innovative Approach. *Remote Sens.* **2022**, *14*, 1565. [CrossRef]
20. Uz, M.; Atman, K.G.; Akyilmaz, O.; Shum, C.K.; Keleş, M.; Ay, T.; Tandoğdu, B.; Zhang, Y.; Mercan, H. Bridging the gap between GRACE and GRACE-FO missions with deep learning aided water storage simulations. *Sci. Total Environ.* **2022**, *830*, 154701. [CrossRef]

21. Lai, Y.; Zhang, B.; Yao, Y.; Liu, L.; Yan, X.; He, Y.; Ou, S. Reconstructing the data gap between GRACE and GRACE follow-on at the basin scale using artificial neural network. *Sci. Total Environ.* **2022**, *823*, 153770. [CrossRef]
22. Li, F.; Kusche, J.; Rietbroek, R.; Wang, Z.; Forootan, E.; Schulze, K.; Lück, C. Comparison of Data-Driven Techniques to Reconstruct (1992–2002) and Predict (2017–2018) GRACE-Like Gridded Total Water Storage Changes Using Climate Inputs. *Water Resour. Res.* **2020**, *56*, e2019WR026551. [CrossRef]
23. Ahi, G.O.; Cekim, H.O. Long-term temporal prediction of terrestrial water storage changes over global basins using GRACE and limited GRACE-FO data. *Acta Geod. Geophys.* **2021**, *56*, 321–344. [CrossRef]
24. Chao, N.; Wang, Z. Characterized Flood Potential in the Yangtze River Basin from GRACE Gravity Observation, Hydrological Model, and In-Situ Hydrological Station. *J. Hydrol. Eng.* **2017**, *22*, 05017016. [CrossRef]
25. Girotto, M.; De Lannoy, G.J.M.; Reichle, R.H.; Rodell, M.; Draper, C.; Bhanja, S.N.; Mukherjee, A. Benefits and pitfalls of GRACE data assimilation: A case study of terrestrial water storage depletion in India. *Geophys. Res. Lett.* **2017**, *44*, 4107–4115. [CrossRef]
26. Vishwakarma, B.D.; Zhang, J.; Sneeuw, N. Downscaling GRACE total water storage change using partial least squares regression. *Sci. Data* **2021**, *8*, 95. [CrossRef]
27. Eicker, A.; Jensen, L.; Wöhnke, V.; Dobslaw, H.; Kvas, A.; Mayer-Gürr, T.; Dill, R. Daily GRACE satellite data evaluate short-term hydro-meteorological fluxes from global atmospheric reanalyses. *Sci. Rep.* **2020**, *10*, 4504. [CrossRef]
28. Wang, F.; Shen, Y.; Chen, T.; Chen, Q.; Li, W. Improved multi-channel singular spectrum analysis for post-processing GRACE monthly gravity field models. *Geophys. J. Int.* **2020**, *223*, 825–839. [CrossRef]
29. Sun, Z.; Long, D.; Yang, W.; Li, X.; Pan, Y. Reconstruction of GRACE data on changes in total water storage over the global land surface and sixty basins. *Water Resour. Res.* **2020**, *56*, e2019WR026250. [CrossRef]
30. Zhong, L.; Sośnica, K.; Weigelt, M.; Liu, B.; Zou, X. Time-Variable Gravity Field from the Combination of HLSST and SLR. *Remote Sens.* **2021**, *13*, 3491. [CrossRef]
31. Save, H.; Bettadpur, S.; Tapley, B.D. High-resolution CSR GRACE RL05 mascons. *J. Geophys. Res. Solid Earth* **2016**, *121*, 7547–7569. [CrossRef]
32. Lenczuk, A.; Leszczuk, G.; Klos, A.; Bogusz, J. Comparing variance of signal contained in the most recent GRACE solutions. *Geod. Cartogr.* **2020**, *69*, 19–37.
33. Rodell, M.; Houser, P.R.; Jambor, U.; Gottschalck, J.; Mitchell, K.; Meng, C.-J.; Arsenault, K.; Cosgrove, B.; Radakovich, J.; Bosilovich, M.; et al. The Global Land Data Assimilation System. *Bull. Am. Meteorol. Soc.* **2004**, *85*, 381–394. [CrossRef]
34. Rodell, M.; Beaudoing, K.H. *GLDAS Noah Land Surface Model L4 Monthly 1.0 × 1.0 Degree, Version 001*; Technical Report; Goddard Earth Sciences Data and Information Services Center (GESDISC): Greenbelt, MD, USA, 2003.
35. Döll, P.; Hoffmann-Dobrev, H.; Portmann, F.T.; Siebert, S.; Eicker, A.; Rodell, M.; Strassberg, G.; Scanlon, B.R. Impact of water withdrawals from groundwater and surface water on continental water storage variations. *J. Geodyn.* **2012**, *59–60*, 143–156. [CrossRef]
36. Friis-Christensen, E.; Lühr, H.; Hulot, G. Swarm: A constellation to study the Earth's magnetic field. *Earth Planets Space* **2006**, *58*, 351–358. [CrossRef]
37. Wang, Z.; Tian, K.; Li, F.; Xiong, S.; Gao, Y.; Wang, L.; Zhang, B. Using Swarm to Detect Total Water Storage Changes in 26 Global Basins (Taking the Amazon Basin, Volga Basin and Zambezi Basin as Examples). *Remote Sens.* **2021**, *13*, 2659. [CrossRef]
38. Humphrey, V.; Gudmundsson, L.; Seneviratne, S.I. Assessing Global Water Storage Variability from GRACE: Trends, Seasonal Cycle, Subseasonal Anomalies and Extremes. *Surv. Geophys.* **2016**, *37*, 357–395. [CrossRef]
39. Box, G.E.P.; Jenkins, G.M. *Time Series Analysis: Forecasting and Control*; Holden-Day: San Francisco, CA, USA, 1976.
40. Akaike, H. Information theory and an extension of the maximum likelihood principle. In *Selected Papers of Hirotugu Akaike*; Parzen, E., Tanabe, K., Kitagawa, G., Eds.; Springer Series in Statistics; Springer: New York, NY, USA, 1998; pp. 199–213.
41. Nash, J.E.; Sutcliffe, J.V. River flow forecasting through conceptual models part I—A discussion of principles. *J. Hydrol.* **1970**, *10*, 282–290. [CrossRef]
42. Getirana, A.; Kumar, S.; Girotto, M.; Rodell, M. Rivers and Floodplains as Key Components of Global Terrestrial Water Storage Variability. *Geophys. Res. Lett.* **2017**, *44*, 10359–10368. [CrossRef]
43. Sun, A.Y. Predicting groundwater level changes using GRACE data. *Water Resour. Res.* **2013**, *49*, 5900–5912. [CrossRef]
44. Scanlon, B.R.; Zhang, Z.; Save, H.; Wiese, D.N.; Landerer, F.W.; Long, D.; Longuevergne, L.; Chen, J. Global evaluation of new GRACE mascon products for hydrologic applications. *Water Resour. Res.* **2016**, *52*, 9412–9429. [CrossRef]
45. Lenczuk, A.; Leszczuk, G.; Klos, A.; Kosek, W.; Bogusz, J. Study on the inter-annual hydrology-induced deformations in Europe using GRACE and hydrological models. *J. Appl. Geod.* **2020**, *14*, 393–403. [CrossRef]
46. Zhang, L.; Dobslaw, H.; Stacke, T.; Güntner, A.; Dill, R.; Thomas, M. Validation of terrestrial water storage variations as simulated by different global numerical models with GRACE satellite observations. *Hydrol. Earth Syst. Sci.* **2017**, *21*, 821–837. [CrossRef]
47. Döll, P.; Flörke, M. *Global-Scale Estimation of Diffuse Groundwater Recharge. Model Tuning to Local Data for Semi-Arid and Arid Regions and Assessment of Climate Change Impact*; Frankfurt Hydrology Paper; Institute of Physical Geography, Frankfurt University: Frankfurt am Main, Germany, 2005.
48. Cheon, S.-H.; Hamlington, B.D.; Reager, J.T.; Chandanpurkar, H.A. Identifying ENSO-related interannual and decadal variability on terrestrial water storage. *Sci. Rep.* **2021**, *11*, 13595. [CrossRef]
49. Nie, W.; Zaitchik, B.F.; Rodell, M.; Kumar, S.V.; Anderson, M.C.; Hain, C. Groundwater Withdrawals Under Drought: Reconciling GRACE and Land Surface Models in the United States High Plains Aquifer. *Water Resour. Res.* **2018**, *54*, 5282–5299. [CrossRef]

50. Gloor, M.; Brienen, R.J.W.; Galbraith, D.; Feldpausch, T.R.; Schöngart, J.; Guyot, J.-L.; Espinoza, J.C.; Lloyd, J.; Phillips, O.L. Intensification of the Amazon hydrological cycle over the last two decades. *Geophys. Res. Lett.* **2013**, *40*, 1729–1733. [CrossRef]
51. Wang, W.; Shen, Y.; Wang, F.; Li, W. Two Severe Prolonged Hydrological Droughts Analysis over Mainland Australia Using GRACE Satellite Data. *Remote Sens.* **2021**, *13*, 1432. [CrossRef]
52. Wouters, B.; Gardner, A.S.; Moholdt, G. Global Glacier Mass Loss During the GRACE Satellite Mission (2002–2016). *Front. Earth Sci.* **2019**, *7*, 96. [CrossRef]
53. Li, F.; Kusche, J.; Chao, N.; Wang, Z.; Löcher, A. Long-Term (1979–Present) Total Water Storage Anomalies Over the Global Land Derived by Reconstructing GRACE Data. *Geophys. Res. Lett.* **2021**, *48*, e2021GL093492. [CrossRef]
54. Zhang, Y.; Dannenberg, M.P.; Hwang, T.; Song, C. El Niño–Southern Oscillation-induced variability of terrestrial gross primary production during the satellite era. *J. Geophy. Res. Biogeosci.* **2019**, *124*, 2419–2431. [CrossRef]
55. García-Herrera, R.; Garrido-Perez, J.M.; Barriopedro, D.; Ordóñez, C.; Vicente-Serrano, S.M.; Nieto, R.; Gimeno, L.; Sorí, R.; Yiou, P. The European 2016/17 Drought. *J. Clim.* **2019**, *32*, 3169–3187. [CrossRef]
56. Boergens, E.; Güntner, A.; Dobslaw, H.; Dahle, C. Quantifying the Central European Droughts in 2018 and 2019 with GRACE-Follow-On. *Geophys. Res. Lett.* **2020**, *47*, e2020GL087285. [CrossRef]
57. Hari, V.; Rakovec, O.; Markonis, Y.; Hanel, M.; Kumar, R. Increased future occurrences of the exceptional 2018–2019 Central European drought under global warming. *Sci. Rep.* **2020**, *10*, 12207. [CrossRef] [PubMed]
58. Zhong, B.; Li, X.; Chen, J.; Li, Q.; Liu, T. Surface Mass Variations from GPS and GRACE/GFO: A Case Study in Southwest China. *Remote Sens.* **2020**, *12*, 1835. [CrossRef]
59. Wang, F.; Shen, Y.; Chen, Q.; Wang, W. Bridging the gap between GRACE and GRACE follow-on monthly gravity field solutions using improved multichannel singular spectrum analysis. *J. Hydrol.* **2021**, *594*, 125972. [CrossRef]
60. Wessel, P.; Luis, J.F.; Uieda, L.; Scharroo, R.; Wobbe, F.; Smith, W.H.F.; Tian, D. The Generic Mapping Tools Version 6. *Geochem. Geophys. Geosyst.* **2019**, *20*, 5556–5564. [CrossRef]